Applied Mathematical Modelling 113 (2023) 528–544

Contents lists available at ScienceDirect

Applied Mathematical Modelling

journal homepage: www.elsevier.com/locate/apm

Saturated and asymmetric saturated impulsive control synchronization of coupled delayed inertial neural networks with time-varying delays

K. Udhayakumar[a], S. Shanmugasundaram[b], Ardak Kashkynbayev[c], K. Janani[b], R. Rakkiyappan[b,*]

[a] Department of Mathematical Sciences, College of Science, UAE University, Al-Ain, United Arab Emirates
[b] Department of Mathematics, Bharathiar University, Coimbatore 641 046, Tamilnadu, India
[c] Department of Mathematics, Nazarbayev University, Nur-Sultan city, Kazakhstan

ARTICLE INFO

Article history:
Received 18 March 2022
Revised 5 September 2022
Accepted 12 September 2022
Available online 16 September 2022

Keywords:
Inertial neural networks
Synchronization
Saturation
Impulsive control
Time-varying delay
Coupling delay

ABSTRACT

This paper considers control systems with impulses that are saturated and asymmetrically saturated which are used to examine the synchronization of inertial neural networks (INNs) with time-varying delay and coupling delays. Under the theoretical discussions, mixed delays, such as transmission delay and coupling delay are presented for inertial neural networks. The addressed INNs are transformed into first order differential equations utilizing variable transformation on INNs and then certain adequate conditions are derived for the exponential synchronization of the addressed model by substituting saturation nonlinearity with a dead-zone function. In addition, an asymmetric saturated impulsive control approach is given to realize the exponential synchronization of addressed INNs in the leader-following synchronization pattern. Finally, simulation results are used to validate the theoretical research findings.

1. Introduction

Neural Networks (NNs) have gained popularity in previous centuries owing to their wide application in various fields, such as frequency image analysis, information processing, financial management sector, data interpretation, optimization problems and classification techniques. These applications are known to significantly rely on dynamical behaviors of NNs [1–9], which is a fundamental property in NN development. The inertial neural network is a neural circuit model that exhibited the inertial nature of a network which has been defined using second-order differential equations. In contrast to the cases discussed in first-order systems, the differential equations defined by second-order INNs can accurately reflect the genetic NN attributes and based on the second derivative have much more complicated dynamical behaviour leading to more practical applications [2,3]. One of the major hot spots in scientific research in recent years has been neural network research. It is vital to research the dynamic behavior of coupled neural networks in order to have some theoretical direction in many engineering applications of neural networks. With a rich research history spanning electronic communication, automatic control, and social science, synchronization of coupled neural networks has significant theoretical and real-world

* Corresponding author.
E-mail address: rakkiyappan.maths@buc.edu.in (R. Rakkiyappan).

https://doi.org/10.1016/j.apm.2022.09.011

implications for the study of nature. For example, in [4] the authors devoted to investigating the synchronization problem of coupled memristive neural networks under event-triggered control for the first time. Finite-time and fixed-time synchronization of a class of coupled discontinuous neural networks is addressed under the framework of Filippov solution in [5]. And by using the theory of differential inclusions and a discontinuous control law finite-time and fixed-time synchronization problem is investigated. By directly constructing the discontinuous complex-valued controllers, fixed-time synchronization of coupled memristive complex-valued neural networks is investigated in [6]. Finite time passivity and finite-time synchronization issues are addressed in [7] for coupled complex-valued memristive neural networks. In particular, impulsive control is characterized by lower control cost, higher confidentiality, and stronger robustness. In order to achieve the desired control performance, we can design the impulsive strength artificially. Since actuator saturation is a common occurrence in almost all control systems, it is actually very challenging from the perspective of applications to accomplish the design aim for each control input. Saturation-related negative behaviors may be seen if such constraints are not treated correctly or even taken into account by the appropriate controllers. Naturally, the influence of saturated impulses must be taken into account when researching the impulsive regulation of coupled neural networks. Compared with the previous results, in this paper, a novel saturated and asymmetric saturated impulsive controllers are designed such that the estimating domain of attraction can be derived, which is one of the main novelty considered in this article.

The fundamentals of NNs include stability, stabilization, state estimation, periodic attractors, robust stability, and so on. Among these, synchronization has experienced significant rise in analysis attention in recent years. It is also a form of collective behaviour to describe a number of environmental occurrences [10–13]. Synchronization is a hot topic in nonlinear dynamical systems research. The major applications of the system in encrypted transmission, biological systems, cognitive processes, etc., has resulted in extensive synchronizing control and numerous positive outcomes [14–16]. Several types of synchronization includes chaotic synchronization, outer synchronization, and cluster synchronization has been investigated from several perspectives [8,17–20]. Synchronization can be accomplished through the use of traditional control mechanisms such as feedback control, backstepping control, intermittent control, impulsive control, sampled-data control, event-triggered control, adaptive control and so on [21–25]. For instance, the authors of [26] achieved exponential synchronization for memristor based neural networks with various delays. Time delay, which is an inherent property of signal transmission between neurons, is one of the primary causes of neural network instability and poor performance. In order to display chaotic events that can be used to secure communication, time delays are included in NNs [27–32]. In [31], the authors considered INNs with time varying delays and achieved multiple finite time synchronization through a unified control scheme. The authors of [2] considered an INN with time varying delay and coupling delay and achieved global asymptotic stability through adaptive control scheme.

In recent years, impulsive control techniques are frequently employed to stabilize and synchronize nonlinear unstable dynamical and chaotic systems as an efficient control means. The primary principle behind impulsive control is to change a system's state whenever certain objectives are fulfilled. Because of the lower control costs, this is the most used method in practice. In light of these advantages, the stability of impulsive neural networks has recently been investigated [26,33–35]. In some kind of broad array of applications, impulse control occurs naturally, as well as for orbit transmission, interruption control, sustainable growth or network synchronization, robotic arm regulate, so on and so forth [28,36,37]. Often researchers concentrated the impulsive controller, because of the possibility of saving the bandwidth of a network, which in the event of systems that are capable by the networks could well reduce the cost of control or network [38,39]. The exponential stability of impulsive control systems with time delay is studied in [40]. The average impulsive interval approach allows for the establishment of some necessary Lyapunov-based requirements for the stability of impulsive time-delay systems. It is interesting to show that some unstable impulsive time-delay systems may be stabilized by increasing the time delay in continuous dynamics. The authors of [41] investigated the exponential stability of nonlinear delayed systems with destabilizing and stabilizing delayed impulses. If the time delays in impulses can be flexible and even larger than the length of impulsive interval, then the stability of delayed systems is obtained with destabilizing delayed impulses, and if the time delays in impulses are flexible between two consecutive impulsive instants the stability of delayed systems is investigated with stabilizing delayed impulses.

The controller's output signal is usually provided to the controlled system through actuator in real-world controllers, and the controlled item is subsequently driven to accomplish the task. Physiological limits realizes the quantity of input signals that the actuator can generate. If the input signal is excessively strong, the output signal from the actuator to the controlled system will be corrupted first. Actuator saturation causes the closed-loop system's performance to drop dramatically. If the saturation limit is not taken into account when designing the control system, it will degrade the system's performance, resulting in lag, increased overshoot, oscillation, and even instability [18,26,42]. Each physical actuator or sensor in control systems is prone to saturation as a result of its upper and lower limits. Saturation nonlinearities are frequently researched systematically in engineering applications such as control systems and NN systems. The evaluation and implementation of a system that has saturation nonlinearities is a major challenge merely because of how they occur. The first technique for dealing with the experimental consequences of saturation is to disregard it during the initial stages of the control design process [43]. To initiate these anti-windup techniques, ad hoc changes and simulations were utilized [44–46]. The actuator is able to stay within its limits as a result of these strategies because it receives more feedback. Many of these methods' stability features, on the other hand, are largely unknown. The second procedure is a little more systematic than the first. It accounts for saturation nonlinearities as part of the control design. The closed-loop system is analysed and the controller is modified in such a way that efficiency is maintained while stability is enhanced, or perhaps the other way around. Characterizing the null controllable region, identifying the set of all states that could be driven to their beginnings by the saturating actuators, and designing validation laws that are justifiable on the entire null controllable region or a large portion of it are all steps in solving actuator saturation with this method. In order to limit the undesirable impacts of the actuator saturation, the dead-zone nonlinearities values must be constructed. We get a saturation impulsive controller term to add, in which an error system will get a value and part of the inequalities will be employed for the reduction. The study and configuration of the system with asymmetric actuator saturation is a critical issue that must be addressed. Asymmetric saturation has been discussed widely in the literature [47–49].

The Lyapunov stability theory is a powerful tool for assessing and designing energy control frameworks. When a definite positive state function is discovered, the system is said to be steady, allowing the time derived along the system's trajectory to be recognized. Motivated by these works, in this article, we intend to achieve exponential synchronization of INNs with time varying and coupling delays via the saturated and asymmetric saturated impulsive control. The major contributions of this article are as follows:

(1) To the best of authors knowledge, this is the first time to investigate the synchronization of INNs with time-varying delay and coupling delays through the saturated and asymmetric saturated impulsive control schemes.
(2) The aforementioned INNs model can be formed into first order differential equations using the variable transformation and some suitable conditions for the exponential synchronization of INNs can be constructed in terms of LMIs by substituting saturation non linearity with a dead-zone function. Furthermore, an asymmetric saturated impulsive control technique was studied to attain the exponential synchronization of addressed INNs in the leader-following synchronization pattern.

The following is a summary of the paper's structure: Section 2 contains the preliminary information as well as a model description of the model under consideration. In Section 3, we examine some results on saturated impulsive control of INNs with delays. Numerical validation to establish the significance of the procured results is detailed out in Section 4. The final section summarizes the entire manuscript to provide a valid conclusion.

2. Preliminaries and model description

Consider the following inertial neural networks (INNs), with both time-varying delay and coupling delay consisting of coupled nodes with each node being a n-dimensional neural network. The dynamics of the i^{th} node is described as:

$$\frac{d^2\omega_i(t)}{dt^2} = -\hat{A}\frac{d\omega_i(t)}{dt} - \hat{B}\omega_i(t) + \hat{C}f(\omega_i(t)) + \hat{D}f(\omega_i(t-\varphi(t))) + I(t) + \sum_{j=1}^{N}\mathscr{H}_{ij}\mathscr{W}\omega_j(t) + \sum_{j=1}^{N}\mathscr{H}_{ij}\bar{\mathscr{W}}\omega_j(t-\sigma(t)) + \nu_i(t), \tag{1}$$

where $i = 1,\dots,N$, the second derivative is called as the inertial term of the INN (1), $\omega_i(t) = (\omega_{i1}(t),\dots,\omega_{in}(t))^T \in \mathbb{R}^n$, is the vector state of the i^{th} node, $\hat{A} = diag\{a_1,\dots,a_n\}, \hat{B} = diag\{b_1,\dots,b_n\}, \hat{C} = \left(c_{pq}\right) \in \mathbb{R}^{n\times n}$ and $\hat{D} = \left(d_{pq}\right) \in \mathbb{R}^{n\times n}$ denotes the connection weight and delayed connection weight matrices respectively. The nonlinear function $f(\omega_i(t)) = (f_1(\omega_{i1}(t)),\dots,f_n(\omega_{in}(t)))^T$ and $f(\omega_i(t-\varphi(t))) = (f_1(\omega_{i1}(t-\varphi(t))),\dots,f_n(\omega_{in}(t-\varphi(t))))^T$is the activation function for the INN (1), $\varphi(t) \in [0,\varphi]$ is the time-varying delay, $I(t) = (I_1(t),\dots,I_n(t))^T$ is the external input, $\mathscr{W} = diag\{\mathscr{W}_1,\dots,\mathscr{W}_n\} > 0$, $\bar{\mathscr{W}} = diag\left\{\bar{\mathscr{W}}_1,\dots,\bar{\mathscr{W}}_n\right\} > 0$ represents the current state and time-varying delay inner coupling matrices respectively. $\mathscr{H} = \left(\mathscr{H}_{ij}\right)_{N\times N}$, $\mathscr{H}_{ij} \le 0$ $(i \ne j)$ and $\mathscr{H}_{ii} = -\sum_{j=1, j\ne i}^{N}\mathscr{H}_{ij}$ is the diagonal element, between the nodes i $(i \ne j)$, the coupling delay is denoted as $\sigma(t) \in [0,\sigma]$ and $\nu_i(t)$ represents the impulsive controller which will be designed in the forthcoming steps. The initial condition of the INN(1) is represented as follows:

$$\omega_i(s) = \xi_i(s),\ \frac{d\omega_i(s)}{ds} = \bar{\xi}_i(s),\ -\varphi \le s \le 0,$$

where $\xi_i(s), \bar{\xi}_i(s)$ are the real valued functions continuous on $[-\varphi, 0]$. Introducing the appropriate variable transformation: $\omega_r(t) = \frac{d\omega_i(t)}{dt} + \omega_i(t)$. The INNs system (1) with the above variable transformation can be reduced into first order ODE as:

$$\begin{cases} \frac{d\omega_i(t)}{dt} = -\omega_i(t) + \omega_r(t) + \nu_{1i}(t), \\ \frac{d\omega_r(t)}{dt} = \mathfrak{A}\omega_i(t) - \mathfrak{B}\omega_r(t) + \hat{C}f(\omega_i(t)) + \hat{D}f(\omega_i(t-\varphi(t))) + I(t) + \sum_{j=1}^{N}\mathscr{H}_{ij}\mathscr{W}\omega_j(t) \\ \qquad + \sum_{j=1}^{N}\mathscr{H}_{ij}\bar{\mathscr{W}}\omega_j(t-\sigma(t)) + \nu_{2i}(t), \end{cases} \tag{2}$$

where $\mathfrak{A} = \hat{A} - \hat{B} - I, \mathfrak{B} = \hat{A} - I, \omega_i(t) = (\omega_{i1}(t),\dots,\omega_{in}(t))^T \in \mathbb{R}^n, \omega_r(t) = (\omega_{r1}(t),\dots,\omega_{rn}(t))^T \in \mathbb{R}^n.$

Define the target desired node in the system INN (1) is described by

$$\frac{d^2h(t)}{dt^2} = -\hat{A}\frac{dh(t)}{dt} - \hat{B}h(t) + \hat{C}f(h(t)) + \hat{D}f(h(t-\varphi(t))) + I(t), \tag{3}$$

and with the help of variable transformation $\frac{dh(t)}{dt} = -h(t) + y(t)$. The compact form of system (3) becomes

$$\begin{cases} \frac{dh(t)}{dt} = -h(t) + y(t), \\ \frac{dy(t)}{dt} = \mathfrak{A}h(t) - \mathfrak{B}y(t) + \hat{C}f(h(t)) + \hat{D}f(h(t-\varphi(t))) + I(t), \end{cases} \tag{4}$$

where $\mathfrak{A} = \hat{A} - \hat{B} - I, \mathfrak{B} = \hat{A} - I, h(t) = (h_1(t), \ldots, h_n(t))^T \in \mathbb{R}^n, y(t) = (y_1(t), \ldots, y_n(t))^T \in \mathbb{R}^n$.

Then the synchronization error between (2) and (4) is described by

$$\begin{cases} \frac{de_{1i}(t)}{dt} = -e_{1i}(t) + e_{2i}(t) + \nu_{1i}(t), \\ \frac{de_{2i}(t)}{dt} = \mathfrak{A}e_{1i}(t) - \mathfrak{B}e_{2i}(t) + \hat{C}f(e_{1i}(t)) + \hat{D}f(e_{1i}(t-\varphi(t))) \\ \qquad +I(t) + \sum_{j=1}^{N} \mathscr{H}_{ij}\mathscr{W}e_{1i}(t) + \sum_{j=1}^{N} \mathscr{H}_{ij}\bar{\mathscr{W}}e_{1i}(t-\sigma(t)) + \nu_{2i}(t), \end{cases} \tag{5}$$

Here, $e_{1i}(t) = \omega_i(t) - h(t), e_{2i}(t) = \omega_r(t) - y(t)$. It is important to note that the impulsive controllers $\nu_{1i}(t), \nu_{2i}(t)$ only knows how to manage the condition of the INNs system (1) associated with a particular point t_k, and for a more effective solution to the problem, the impusive controller is designed as follows:

$$\nu_{1i}(t) = \sum_{k=1}^{\infty} \vartheta_{1i}(t)\delta(t-t_k), \nu_{2i}(t) = \sum_{k=1}^{\infty} \vartheta_{2i}(t)\delta(t-t_k), t \in [t_k, t_{k+1}),$$

where $k \in \mathbb{Z}_+, \vartheta_{1i}(t) = \mathfrak{K}_1 e_{1i}(t), \vartheta_{2i}(t) = \mathfrak{K}_1 e_{2i}(t), \mathfrak{K}_1, \mathfrak{K}_2 \in \mathbb{R}^{n\times n}$ is the impulsive control gain and $\delta(.)$ is the delta function with sequence $\{t_k, k \in \mathbb{Z}_+\}$ satisfying $0 = t_0 < t_1 < \ldots < t_k \ldots < \ldots, \lim_{k\to\infty} t_k = \infty$. Moreover, in procedure, the magnitude of the signal that a control system can produce is generally defined as physical or protection constraints, making reach desired effectiveness unrealistic. To effectively address this problem, the impulsive controller with actuator saturation is presented as:

$$\nu_{1i}(t) = \sum_{k=1}^{\infty} sat(\vartheta_{1i}(t))\delta(t-t_k), \nu_{2i}(t) = \sum_{k=1}^{\infty} sat(\vartheta_{2i}(t))\delta(t-t_k), t \in [t_k, t_{k+1}), \tag{6}$$

where $sat(\vartheta_{1i}(t)) = (sat(\vartheta_{1i1}(t)), \ldots, sat(\vartheta_{1in}(t)))^T, sat(\vartheta_{2i}(t)) = (sat(\vartheta_{2i1}(t)), \ldots, sat(\vartheta_{2in}(t)))^T$ denotes the saturation function. By the above equation, the saturated impulsive controller (6) defined with the synchronization error system is undertaken as:

$$\begin{cases} \frac{de_{1i}(t)}{dt} = -e_{1i}(t) + e_{2i}(t), \\ \frac{de_{2i}(t)}{dt} = \mathfrak{A}e_{1i}(t) - \mathfrak{B}e_{2i}(t) + \hat{C}f(e_{1i}(t)) + \hat{D}f(e_{1i}(t-\varphi(t))) \\ \qquad +I(t) + \sum_{j=1}^{N} \mathscr{H}_{ij}\mathscr{W}e_{1i}(t) + \sum_{j=1}^{N} \mathscr{H}_{ij}\bar{\mathscr{W}}e_{1i}(t-\sigma(t)), \\ \triangle e_{1i}(t_k) = sat(\mathfrak{K}_1 e_{1i}(t_k^-)), \triangle e_{2i}(t_k) = sat(\mathfrak{K}_2 e_{2i}(t_k^-)), k \in \mathbb{Z}_+, \\ e_{1i}(s) = \chi_{1i}(s), e_{2i}(s) = \chi_{2i}(s), s \in [t_0 - h, t_0]. \end{cases} \tag{7}$$

Let us construct the dead-zone non linearity $dz(\mathfrak{K}_1 e_{1i}(t))$ and $dz(\mathfrak{K}_2 e_{2i}(t))$ defined as

$dz(\mathfrak{K}_1 e_{1i}(t)) = \mathfrak{K}_1 e_{1i}(t) - sat(\mathfrak{K}_1 e_{1i}(t))$ and $dz(\mathfrak{K}_2 e_{2i}(t)) = \mathfrak{K}_2 e_{2i}(t) - sat(\mathfrak{K} e_{2i}(t))$ to reduce the undesirable effects induced by actuator saturation. Then the error system (7) can be rewritten as follows:

$$\begin{cases} \frac{de_{1i}(t)}{dt} = -e_{1i}(t) + e_{2i}(t), \\ \frac{de_{2i}(t)}{dt} = \mathfrak{A}e_{1i}(t) - \mathfrak{B}e_{2i}(t) + \hat{C}f(e_{1i}(t)) + \hat{D}f(e_{1i}(t-\varphi(t))) \\ \qquad +I(t) + \sum_{j=1}^{N} \mathscr{H}_{ij}\mathscr{W}e_{1i}(t) + \sum_{j=1}^{N} \mathscr{H}_{ij}\bar{\mathscr{W}}e_{1i}(t-\sigma(t)), \\ e_{1i}(t_k) = (I_n + \mathfrak{K}_1)e_{1i}(t_k^-) - dz(\mathfrak{K}_1 e_{1i}(t_k^-)), \\ e_{2i}(t_k) = (I_n + \mathfrak{K}_2)e_{2i}(t_k^-) - dz(\mathfrak{K}_2 e_{2i}(t_k^-)), k \in \mathbb{Z}_+, \\ e_{1i}(s) = \xi_{1i}(s), e_{2i}(s) = \xi_{2i}(s), s \in [t_0 - h, t_0]. \end{cases} \tag{8}$$

Remark 2.1. When the continuous delayed neural network is exponentially stable but the impulses are input disturbances, sufficient conditions for exponential stability concerning the magnitude and frequency of the impulses are derived in order to maintain the original neural networks exponential stability. When the continuous neural network is unstable, sufficient stability conditions that utilize impulsive effects to stabilize the unstable neural network are given.

Assumption 2.2. If the activation functions $f_p(\cdot) : \mathbb{R} \to \mathbb{R}$ satisfy the Lipschitz condition, then there exists a positive constant F_p such that $|f_p(x) - f_p(y)| \le F_p|x-y|$ for all $x, y \in \mathbb{R}, 1 \le p \le n$.

Lemma 2.3. [43] *Consider a matrix $K \in R^{n\times n}$ such that $e = [e_1^T, e_2^T, \dots, e_N^T]^T$ represents the diagonal element, if $e \in L(H)$, then the positive definite matrix $F \in R^{n\times n}$, the subsequent inequality holds $\Gamma(Ke_i)^T F(\Gamma(Ke_i) - \mathscr{N} e_i) \le 0, i \in N$.*

Lemma 2.4. [43] *(Matrix Cauchy Inequality) Suppose that $Q > 0$ represents a symmetric positive definite matrix and C and D are real matrices with suitable aspects, the following inequality holds:*

$$C^T D + D^T C \le C^T QC + D^T Q^{-1} D.$$

Lemma 2.5. [43] *Let $0 \le \varphi(t) \le \varphi, 0 \le \sigma(t) \le \sigma$, and $h = \varphi \vee \sigma$. If there exist positive constants $\alpha_1, \alpha_2, \alpha_3$ and $\gamma > 0$ such that*

$$\begin{cases} D^+\mathfrak{a}(t) \le \alpha_1\mathfrak{a}(t) + \alpha_2\mathfrak{a}(t-\varphi(t)) + \alpha_3\mathfrak{a}(t-\sigma(t)), & t \ne t_k, t \ge t_0, \\ \mathfrak{a}(t_k) \le \gamma\mathfrak{a}(t_k^-), & k \in \mathbb{Z}_+, \end{cases}$$

$$\begin{cases} D^+\mathfrak{b}(t) > \alpha_1\mathfrak{b}(t) + \alpha_2\mathfrak{b}(t-\varphi(t)) + \alpha_3\mathfrak{b}(t-\sigma(t)), t \ne t_k, & t \ge t_0, \\ \mathfrak{b}(t_k) = \gamma\mathfrak{b}(t_k^-), & k \in \mathbb{Z}_+, \end{cases}$$

then $\mathfrak{a}(t) \le \mathfrak{b}(t)$ for $t \in [t_0 - h, t_0]$ implies that $\mathfrak{a}(t) \le \mathfrak{b}(t), \forall t \ge t_0$, where functions $\mathfrak{a}(t), \mathfrak{b}(t) \in PC([t_0 - h, +\infty), \mathbb{R}_+)$.

Definition 2.6. [43] The average impulsive interval of the impulsive sequences $\{t_k\}, k \in \mathbb{Z}_+$ is less than T_a, if there exist a positive number T_a and a positive integer $\aleph_0$ such that

$$\aleph(T, s) \ge \frac{T - s}{T_a} - \aleph_0, \forall T \ge s \ge t_0,$$

where $\aleph(T, s)$ denotes the number of impulsive times of the impulsive sequences at t_k occurring on the interval (T, s) and $T_a > 0$ represent the average impulsive interval.

Lemma 2.7. [50] *Let $v \in R^n, \omega \in R^n, \theta \in R_+^n$ and diagonal matrix $S > 0, S \in R^{n\times n}$. Suppose $-\theta_i \le v_i - \omega_i \le \theta_i, i = 1, 2, \cdots, n$, then the inequality $\varphi(v)^T S(\varphi(v) + \omega) \le 0$ is satisfied by the non linearity function $\varphi(v) = \mathrm{sat}(v) - v$.*

Remark 2.8. There have been no relevant exponential synchronization results for coupled delayed INNs using both saturated and asymmetric saturated impulsive control till now. To bridge that gap, we will present many new results in this article that guarantee exponential synchronization of coupled delayed INNs. A saturated and asymmetric saturated impulsive control strategy is proposed to handle this problem. The NNs in this article have an inertial term which is an extension of the earlier papers [43,46,51,52] that did not have an inertial term.

3. Main results

A class of controllers with impulses that incorporate structures with saturation and are described in terms of LMIs are investigated here.

Theorem 3.1. *Suppose that there exist constants $\alpha_1 > 0, \alpha_2 > 0, \alpha_3 > 0, \alpha_4 > 0, \alpha_5 = \max\{\alpha_1, \alpha_2\}$ and some $n \times n$ diagonal matrices $P_1 > 0, P_2 > 0, M > 0, Z_1 > 0, Z_2 > 0, Z_3 > 0$, $n \times n$ matrices $F_1 > 0, F_2 > 0$, $0 < \psi_1, \psi_2 < 1$ and $\aleph \in \max\{\psi_1, \psi_2\}$ such that $I_N \otimes \left(M^T Z_2 M - \alpha_3 P_1 - \alpha_3 P_2\right) \le 0, I_N \otimes (Z_3 - \alpha_4 P_1 - \alpha_4 P_2) \le 0$ and*

$$I_N \otimes \left(2P_1 - P_1 M + M^T Z_1 M + P_2 \mathfrak{A}\delta^{-1} + (\mathscr{H} \otimes P_2 \mathscr{W})\varsigma^{-1} - \alpha_1 P_1\right) \le 0, \tag{9}$$

$$I_N \otimes \left(P_1 M^{-1} + P_2\mathfrak{A}\delta - 2P_2\mathfrak{B} + P_2\hat{C}Z_1^{-1}\hat{C}^T P_2 + P_2\hat{D}Z_2^{-1}\hat{D}^T P_2 + (\mathscr{H} \otimes P_2\mathscr{W})\varsigma + \left(\mathscr{H}\mathscr{H}^T \otimes P_2\bar{\mathscr{W}}Z_3^{-1}\bar{\mathscr{W}}P_2\right) - \alpha_1 P_2\right) \le 0, \tag{10}$$

$$\Delta_1 = \begin{bmatrix} (I_n + \mathfrak{K})^T P_1 (I_n + \mathfrak{K}) - \psi_1 P_1 & (I_n + \mathfrak{K})^T P_1 - \Gamma^T F_1 \\ \star & P_1 - 2F_1 \end{bmatrix} \le 0, \tag{11}$$

$$\Delta_2 = \begin{bmatrix} (I_n + \mathfrak{K})^T P_2 (I_n + \mathfrak{K}) - \psi_2 P_2 & (I_n + \mathfrak{K})^T P_2 - \Gamma^T F_1 \\ \star & P_2 - 2F_2 \end{bmatrix} \le 0, \tag{12}$$

then the error system's (6) trajectory converges to zero exponentially.

Proof: A Lyapunov functional candidate is constructed as follows

$$\mathscr{V}(t) = \mathscr{V}_1(t) + \mathscr{V}_2(t), \tag{13}$$

where $\mathscr{V}_1(t) = \sum_{i=1}^{N} e_{1i}^T(t) P_1 e_{1i}(t), \mathscr{V}_2(t) = \sum_{i=1}^{N} e_{2i}^T(t) P_2 e_{2i}(t)$.

The derivative of $\mathscr{V}(t)$ is taken along the trajectories of (6)

$$
\begin{aligned}
D^{+}\mathscr{V}_1(t) =& 2\sum_{i=1}^{N} e_{1i}^{T}(t)P_1\dot{e}_{1i}(t),\\
=& -2\sum_{i=1}^{N} e_{1i}^{T}(t)P_1 e_{1i}(t) + 2\sum_{i=1}^{N} e_{1i}^{T}(t)P_1 e_{2i}(t),\\
\leq& -2\sum_{i=1}^{N} P_1 e_{1i}^{T}(t)e_{1i}(t) + \sum_{i=1}^{N} P_1 e_{1i}^{T}(t)Me_{1i}(t) + \sum_{i=1}^{N} P_1 e_{2i}^{T}(t)M^{-1}e_{2i}(t),\\
D^{+}\mathscr{V}_2(t) =& 2\sum_{i=1}^{N} e_{2i}^{T}(t)P_2\dot{e}_{2i}(t),\\
=& 2\sum_{i=1}^{N} e_{2i}^{T}(t)P_2\Bigg(\mathfrak{A}e_{1i}(t) - \mathfrak{B}e_{2i}(t) + \hat{C}f(e_{1i}(t)) + \hat{D}f(e_{1i}(t-\varphi(t))) + I(t) + \sum_{j=1}^{N}\mathscr{H}_{ij}\mathscr{W}e_{1i}(t)\\
&+ \sum_{j=1}^{N}\mathscr{H}_{ij}\bar{\mathscr{W}}e_{1i}(t-\sigma(t))\Bigg),\\
=& 2\sum_{i=1}^{N} e_{2i}^{T}(t)P_2\mathfrak{A}e_{1i}(t) - 2\sum_{i=1}^{N} e_{2i}^{T}(t)P_2\mathfrak{B}e_{2i}(t) + 2\sum_{i=1}^{N} e_{2i}^{T}(t)P_2\hat{C}f(e_{1i}(t)) + 2\sum_{i=1}^{N} e_{2i}^{T}(t)P_2\hat{D}f(e_{1i}(t-\varphi(t)))\\
&+ 2\sum_{i=1}^{N} e_{2i}^{T}(t)P_2\sum_{j=1}^{N}\mathscr{H}_{ij}\mathscr{W}e_{1i}(t) + 2e_{2i}^{T}(t)P_2\sum_{j=1}^{N}\mathscr{H}_{ij}\bar{\mathscr{W}}e_{1i}(t-\sigma(t)).
\end{aligned}
$$

By matrix cauchy inequality,

$$
\begin{aligned}
2e_{2i}^{T}(t)P_2\hat{C}f(e_{1i}(t)) \leq& e_{2i}^{T}(t)P_2\hat{C}Z_1^{-1}\hat{C}^{T}P_2e_{2i}(t) + f^{T}(e_{1i}(t))Z_1f(e_{1i}(t)),\\
\leq& e_{2i}^{T}(t)P_2\hat{C}Z_1^{-1}\hat{C}^{T}P_2e_{2i}(t) + e_{1i}^{T}(t)M^{T}Z_1Me_{1i}(t),\\
2e_{2i}^{T}(t)P_2\hat{D}f(e_{1i}(t-\varphi(t))) \leq& e_{2i}^{T}(t)P_2\hat{D}Z_2^{-1}\hat{D}^{T}P_2e_{2i}(t) + f^{T}(e_{1i}(t-\varphi(t)))Z_2f(e_{1i}(t-\varphi(t))),\\
\leq& e_{2i}^{T}(t)P_2\hat{D}Z_2^{-1}\hat{D}^{T}P_2e_{2i}(t) + e_{1i}^{T}(t-\varphi(t))M^{T}Z_2Me_{1i}(t-\varphi(t)).
\end{aligned}
$$

The coupled terms becomes

$$
\begin{aligned}
2\sum_{i=1}^{N} e_{2i}^{T}(t)P_2\sum_{j=1}^{N}\mathscr{H}_{ij}\mathscr{W}e_{1i}(t) =& 2e_2^{T}(t)P_2(\mathscr{H}\otimes P_2\mathscr{W})e_1(t),\\
2\sum_{i=1}^{N} e_{2i}^{T}(t)P_2\sum_{j=1}^{N}\mathscr{H}_{ij}\bar{\mathscr{W}}e_{1i}(t-\sigma(t)) =& 2e_2^{T}(t)P_2\left(\mathscr{H}\otimes P_2\bar{\mathscr{W}}\right)e_1(t-\sigma(t)),\\
=& e_2^{T}(t)\left(\mathscr{H}\mathscr{H}^{T}\otimes P_2\bar{\mathscr{W}}Z_3^{-1}\bar{\mathscr{W}}P_2\right)e_2(t) + e_1^{T}(t-\sigma(t))(I_N\otimes Z_3)e_1(t-\sigma(t)).
\end{aligned}
$$

$$
\begin{aligned}
D^{+}\mathscr{V}(t) =& D^{+}\mathscr{V}_1(t) + D^{+}\mathscr{V}_2(t)\\
=& 2\sum_{i=1}^{N} P_1e_{1i}^{T}(t)e_{1i}(t) - \sum_{i=1}^{N} P_1Me_{1i}^{T}(t)e_{1i}(t) + \sum_{i=1}^{N} P_1M^{-1}e_{2i}^{T}(t)e_{2i}(t) + \sum_{i=1}^{N} P_2\mathfrak{A}\delta e_{2i}^{T}(t)e_{2i}(t),\\
&+ \sum_{i=1}^{N} P_2\mathfrak{A}\delta^{-1}e_{1i}^{T}(t)e_{1i}(t) - 2\sum_{i=1}^{N} P_2\mathfrak{B}e_{2i}^{T}(t)e_{2i}(t) + \sum_{i=1}^{N} e_{2i}^{T}(t)P_2\hat{C}Z_1^{-1}\hat{C}^{T}P_2e_{2i}(t) + \sum_{i=1}^{N} e_{1i}^{T}(t)M^{T}Z_1Me_{1i}(t)\\
&+ \sum_{i=1}^{N} e_{2i}^{T}(t)P_2\hat{D}Z_2^{-1}\hat{D}^{T}P_2e_{2i}(t) + \sum_{i=1}^{N} e_{1i}^{T}(t-\varphi(t))M^{T}Z_2Me_{1i}(t-\varphi(t)) + e_2^{T}(\mathscr{H}\otimes P_2\mathscr{W})\varsigma(t)e_2(t)\\
&+ e_1^{T}(t)(\mathscr{H}\otimes P_2\mathscr{W})\varsigma^{-1}e_1(t) + e_2^{T}(t)\left(\mathscr{H}\mathscr{H}^{T}\otimes P_2\bar{\mathscr{W}}Z_3^{-1}\bar{\mathscr{W}}P_2\right)e_2(t) + e_1^{T}(t-\sigma(t))(I_N\otimes Z_3)e_1(t-\sigma(t)),\\
=& e_1^{T}(t)\left[I_N\otimes\left(2P_1 - P_1M + M^{T}Z_1M + P_2\mathfrak{A}\delta^{-1} + (\mathscr{H}\otimes P_2\mathscr{W})\varsigma^{-1} - \alpha_1P_1 - \alpha_1P_2\right)\right]e_1(t)\\
&+ e_2^{T}(t)\Big[I_N\otimes\Big(P_1M^{-1} + P_2\mathfrak{A}\delta - 2P_2\mathfrak{B} + P_2\hat{C}Z_1^{-1}\hat{C}^{T}P_2 + P_2\hat{D}Z_2^{-1}\hat{D}^{T}P_2 + (\mathscr{H}\otimes P_2\mathscr{W})\varsigma\\
&+ \left(\mathscr{H}\mathscr{H}^{T}\otimes P_2\bar{\mathscr{W}}Z_3^{-1}\bar{\mathscr{W}}P_2\right) - \alpha_2P_1 - \alpha_2P_2\Big)\Big]e_2(t)
\end{aligned}
$$

$$
\begin{aligned}
&+e_1^T(t-\varphi(t))\Big[I_N\otimes\Big(M^TZ_2M-\alpha_3P_1-\alpha_3P_2\Big)\Big]e_1(t-\varphi(t))\\
&+e_1^T(t-\sigma(t))[I_N\otimes(Z_3-\alpha_4P_1-\alpha_4P_2)]e_1(t-\sigma(t))+e_1^T(t)\alpha_1P_1e_1(t)+e_2^T(t)\alpha_1P_2e_2(t)\\
&+e_1^T(t)\alpha_2P_1e_1(t)+e_2^T(t)\alpha_2P_2e_2(t)+e_1^T(t-\varphi(t))\alpha_3P_1e_1(t-\varphi(t))+e_2^T(t-\varphi(t))\alpha_3P_2e_2(t-\varphi(t))\\
&+e_1^T(t-\sigma(t))\alpha_4P_1e_1(t-\sigma(t))+e_2^T(t-\sigma(t))\alpha_4P_2e_2(t-\sigma(t)),\\
&\le\alpha_1\mathscr{V}(t)+\alpha_2\mathscr{V}(t)+\alpha_3\mathscr{V}(t-\varphi(t))+\alpha_4\mathscr{V}(t-\sigma(t)).
\end{aligned}
\tag{14}
$$

When $t=t_k$,

$$
\begin{aligned}
\mathscr{V}(t_k)&=\mathscr{V}_1(t_k)+\mathscr{V}_2(t_k),\\
&=\sum_{i=1}^N e_{1i}^T(t_k)P_1e_{1i}(t_k)+\sum_{i=1}^N e_{2i}^T(t_k)P_2e_{2i}(t_k),\\
&\le\sum_{i=1}^N e_{1i}^T(t_k^-)(I_n+\Re)^TP_1(I_n+\Re)e_{1i}(t_k^-)-\sum_{i=1}^N dz^T(\Re e_{1i}(t_k^-))P_1e_{1i}(t_k^-)\\
&\quad+\sum_{i=1}^N e_{1i}^T(t_k^-)(I_n+\Re)^TP_1(-dz(\Re e_{1i}(t_k^-)))+\sum_{i=1}^N dz^T(\Re e_{1i}(t_k^-))P_1dz(\Re e_{1i}(t_k^-))\\
&\quad+\sum_{i=1}^N e_{2i}^T(t_k^-)(I_n+\Re)^TP_2(I_n+\Re)e_{2i}(t_k^-)-\sum_{i=1}^N dz^T(\Re e_{2i}(t_k^-))P_2e_{2i}(t_k^-)\\
&\quad+\sum_{i=1}^N e_{2i}^T(t_k^-)(I_n+\Re)^TP_2(-dz(\Re e_{2i}(t_k^-)))+\sum_{i=1}^N dz^T(\Re e_{2i}(t_k^-))P_2dz(\Re e_{2i}(t_k^-))\\
&\quad-2\sum_{i=1}^N dz^T\big(\Re e_{1i}\big(t_k^-\big)\big)F_1\big[dz\big(\Re e_{1i}\big(t_k^-\big)\big)-\Gamma e_{1i}\big(t_k^-\big)\big]\\
&\quad-2\sum_{i=1}^N dz^T\big(\Re e_{2i}\big(t_k^-\big)\big)F_2\big[dz\big(\Re e_{2i}\big(t_k^-\big)\big)-\Gamma e_{2i}\big(t_k^-\big)\big],\\
&\le\sum_{i=1}^N \beta_{1i}^T\big(t_k^-\big)\Theta_1\beta_{1i}\big(t_k^-\big)+\sum_{i=1}^N \beta_{1i}^T\big(t_k^-\big)\Theta_1\beta_{1i}\big(t_k^-\big)-2\sum_{i=1}^N dz^T\big(\Re e_{1i}\big(t_k^-\big)\big)F_1\big[dz\big(\Re e_{1i}\big(t_k^-\big)\big)-\Gamma e_{1i}\big(t_k^-\big)\big]\\
&\quad-2\sum_{i=1}^N dz^T\big(\Re e_{2i}\big(t_k^-\big)\big)F_2\big[dz\big(\Re e_{2i}\big(t_k^-\big)\big)-\Gamma e_{2i}\big(t_k^-\big)\big],\\
&=\sum_{i=1}^N \beta_{1i}^T\big(t_k^-\big)\Delta_1\beta_{1i}\big(t_k^-\big)+\psi_1\mathscr{V}_1\big(t_k^-\big)+\sum_{i=1}^N \beta_{2i}^T\big(t_k^-\big)\Delta_2\beta_{2i}\big(t_k^-\big)+\psi_2\mathscr{V}_2\big(t_k^-\big),\\
&\le\aleph\mathscr{V}(t_k^-),
\end{aligned}
\tag{15}
$$

where

$$
\beta_{1i}\big(t_k^-\big)=\Big[e_{1i}^T\big(t_k^-\big)-dz^T\big(\Re e_{1i}\big(t_k^-\big)\big)\Big]^T\beta_{2i}\big(t_k^-\big)=\Big[e_{2i}^T\big(t_k^-\big)-dz^T\big(\Re e_{2i}\big(t_k^-\big)\big)\Big]^T,\aleph=\max\{\psi_1,\psi_2\}
$$

$$
\Theta_1=\begin{bmatrix}(I_n+\Re)^TP_1(I_n+\Re) & (I_n+\Re)^TP_1\\ \star & P_1\end{bmatrix},\Theta_2=\begin{bmatrix}(I_n+\Re)^TP_2(I_n+\Re) & (I_n+\Re)^TP_2\\ \star & P_2\end{bmatrix}
$$

Consider the following system with the comparison of (10) and (13)

$$
\begin{cases}
D^+v(t)=\alpha_5v_1(t)+\alpha_3v_1(t-\varphi(t))+\alpha_4v_1(t-\sigma(t))+\rho,t\neq t_k,\\
v(t_k)=\ \ \aleph v(t_k^-),t=t_k,\\
v(s)=\ \ \mathscr{V}(s),t_0\le s\le t_0.
\end{cases}
$$

When $s\in[t_0-h,t_0]$, $v(s)\ge\mathscr{V}(s)\ge0$, $\rho>0$ is a constant. By the formula for the variation of parameter, one obtains from the above equation that

$$
v_{\epsilon1}(t)=\zeta(t,t_0)v_{\epsilon1}(t_0)+\int_{t_0}^t\zeta(t,s)(\alpha_3v_{\epsilon1}(s-\varphi(s))+\alpha_4v_{\epsilon1}(s-\sigma(s))+\rho)ds,
$$

where $\zeta(t,s)(t,s>0)$ is the Cauchy matrix for the linear system considered below is given as.

$$
\begin{aligned}
\dot{w}(t)=&\alpha_5w(t),t\neq t_k,\\
w(t_k)=&\aleph w(t_k^-),t=t_k,k\in\mathbb{Z}_+.
\end{aligned}
$$

Now we can formulate the following estimate through the Cauchy matrix representation and by the Definition 2.5, we get

$$\begin{aligned}\zeta(t,s) =& \aleph^{\aleph(t,s)} e^{\alpha_5(t-s)},\\ \leq& \aleph^{\frac{t-s}{T_a}-\aleph_0} e^{\alpha_5(t-s)},\\ =& \aleph^{-\aleph_0} e^{\bar{\alpha}(t-s)}.\end{aligned}$$

where $\bar{\alpha} = \alpha_5 + (ln\aleph/T_a) < 0$. Let $\bar{\nu}_{\epsilon 1} = \sup_{t_0-h\leq s\leq t_0} \mathscr{V}(s)$ and $\kappa = \aleph^{-\aleph_0}\bar{\nu}_{\epsilon 1}$ which leads to

$$\nu_{\epsilon 1}(t) = \kappa e^{\bar{\alpha}(t-t_0)} + \int_{t_0}^{t} \aleph^{-\aleph_0} e^{\bar{\alpha}(t-s)} (\alpha_3 \nu_{\epsilon 1}(s-\varphi(s)) + \alpha_4 \nu_{\epsilon 1}(s-\sigma(s)) + \rho) ds.$$

Define $Z(\theta) = \theta + \aleph^{-\aleph_0}\left(\alpha_3 e^{\varphi\theta} + \alpha_4 e^{\sigma\theta}\right) + \bar{\alpha}$. If $\theta = 0$, then $z(0) = \aleph^{-\aleph_0}(\alpha_3+\alpha_4) + \bar{\alpha} < 0, Z(+\infty) = +\infty$ and $\dot{Z}(\theta) = 1 + \aleph^{-\aleph_0}\left(\varphi\alpha_3 e^{\varphi\theta} + \sigma\alpha_4 e^{\sigma\theta}\right) > 0$. As a result, a unique positive constant θ exists satisfying the condition $\theta + \aleph^{-\aleph_0}\left(\alpha_3 e^{\varphi\theta} + \alpha_4 e^{\sigma\theta}\right) + \bar{\alpha} = 0$. In the following, we show that for all $t_0 \geq t_0 - h$,

$$\nu_{\epsilon 1} = \kappa e^{-\theta(t-t_0)} - \frac{\rho}{\bar{\alpha}\aleph^{\aleph_0} + \alpha_3 + \alpha_4}. \tag{16}$$

For $t \in [t_0 - h, t_0]$, in view of $\aleph^{\aleph_0} > 1$, we have

$$\begin{aligned}\nu_{\epsilon 1}(t) =& \mathscr{V}(t) \leq \bar{\nu}_{\epsilon 1} < \aleph^{-\aleph_0}\bar{\nu}_{\epsilon 1} = \kappa,\\ <& \kappa e^{-\theta(t-t_0)} - \frac{\rho}{\bar{\alpha}\aleph^{\aleph_0} + \alpha_3 + \alpha_4}.\end{aligned} \tag{17}$$

For $t \in (t_0, +\infty)$, we need to prove the following inequality, for $t > 0$.

So we define $\bar{t} = \inf\left\{t > t_0 : \nu_{\epsilon 1}(t) \leq \kappa e^{-\theta(t-t_0)} - \frac{\rho}{\bar{\alpha}\aleph^{\aleph_0} + \alpha_3 + \alpha_4}\right\}$. We assert that the point $\bar{t}$ is impulsive.

From $Z(\theta) = 0$, it is obvious that

$$\begin{aligned}\nu_{\epsilon 1}(\bar{t}) \leq& \kappa e^{\bar{\alpha}(t-t_0)} + \int_{t_0}^{t} \aleph^{-\aleph_0} e^{\bar{\alpha}(t-s)} (\alpha_3 \nu_{\epsilon 1}(s-\varphi(s)) + \alpha_4 \nu_{\epsilon 1}(s-\sigma(s)) + \rho) ds,\\ \leq& \kappa e^{\bar{\alpha}(\bar{t}-t_0)} + \int_{t_0}^{t} \aleph^{-\aleph_0} e^{\bar{\alpha}(t-s)} \left[\alpha_3\left(\kappa e^{-\theta(s-\varphi-t_0)} - \frac{\rho}{\bar{\alpha}\aleph^{\aleph_0} + \alpha_3 + \alpha_4}\right)\right.\\ &\left. + \alpha_4\left(\kappa e^{-\theta(s-\sigma-t_0)} - \frac{\rho}{\bar{\alpha}\aleph^{\aleph_0} + \alpha_3 + \alpha_4}\right) + \rho\right] ds,\\ =& \kappa e^{\bar{\alpha}(\bar{t}-t_0)} + \frac{\kappa\aleph^{-\aleph_0}\alpha_3 e^{\varphi\theta}}{-(\bar{\alpha}+\theta)}\left(e^{-\theta(\bar{t}-t_0)} - e^{-\alpha(\bar{t}-t_0)}\right) + \frac{\kappa\aleph^{-\aleph_0}\alpha_4 e^{\varphi\theta}}{-(\bar{\alpha}+\theta)}\left(e^{-\theta(\bar{t}-t_0)} - e^{-\alpha(\bar{t}-t_0)}\right)\\ &- \frac{\rho}{\bar{\alpha}\aleph^{\aleph_0} + \alpha_3 + \alpha_4}\left(1 - e^{-\alpha(\bar{t}-t_0)}\right),\\ <& \kappa e^{\bar{\alpha}(\bar{t}-t_0)} + \frac{\kappa\aleph^{-\aleph_0}\left(\alpha_3 e^{\varphi\theta} + \alpha_4 e^{\sigma\theta}\right)}{-(\bar{\alpha}+\theta)}\left(e^{-\theta(\bar{t}-t_0)} - e^{-\alpha(\bar{t}-t_0)}\right) - \frac{\rho}{\bar{\alpha}\aleph^{N_0} + \alpha_3 + \alpha_4},\\ =& \kappa e^{-\theta(\bar{t}-t_0)} - \frac{\rho}{\bar{\alpha}\aleph^{\aleph_0} + \alpha_3 + \alpha_4},\end{aligned}$$

which contradicts with the above condition (16). Then let $\rho \to 0^+$ it is obvious to get $\nu_{\epsilon 1}(\bar{t}) \leq \kappa e^{-\theta(\bar{t}-t_0)}$. Noting that $\bar{t} > t_0$, it is easy to obtain that

$$\begin{aligned}\mathscr{V}(\bar{t}) \leq& \nu_{\varepsilon 1}(\bar{t}),\\ \leq& \kappa e^{-\theta\left(\bar{t}-t_0\right)},\\ =& \aleph^{-\aleph_0}\bar{\nu}_{\varepsilon 1} e^{-\theta\left(\bar{t}-t_0\right)},\\ <& \aleph^{-\aleph_0},\end{aligned} \tag{18}$$

which negates the equation $\mathscr{V}(\bar{t}) = \aleph^{-\aleph_0}$. The set inclusion constraint is important in estimating the domain of attraction when studying systems with saturation structure. However, it is based on the fact that the system's trajectory is continuous. The traditional set inclusion constraint is infeasible when the system is subject to impulses. To address this issue, a new set inclusion constraint for impulsive synchronization is developed, that is $\rho(I_N \otimes P, 1) \subset \rho(I_N \otimes P, \aleph^{-\aleph_0}) \subset L(H)$. It should be noted that the restriction $\rho(I_N \otimes P, \aleph^{-\aleph_0}) \subset L(H)$ is required to ensure that the system's trajectory stays within the bounds of $\rho(I_N \otimes P, \aleph^{-\aleph_0})$ on both the continuous intervals and the impulse instants. Therefore, based on the previous discussions, for all $t \geq t_0 - h$, $\mathscr{V}(t) \leq \aleph^{-\aleph_0}\bar{\nu}_{\varepsilon 1} e^{-\theta(t-t_0)}$ i.e,

$$\|e(t)\| \leq \sqrt{\frac{\lambda_{\max}(P)}{\lambda_{\min}(P)\aleph^{\aleph_0}} \sup_{t_0-h\leq s\leq t_0} \sum_{i=1}^{N} \|\chi_i(s)\|^2 e^{-\frac{\theta}{2}(t-t_0)}}, \tag{19}$$

where, $e(t) = (e_1^T(t), e_2^T(t))^T, P = diag(P_1, P_2)^T, \chi \in \rho(I_N \otimes P, 1)$. By using Definition 2.5 as a hint, we can determine that the coupled delayed neural network (2) is exponentially synced to the isolated node (3). The proof is now completed.

Remark 3.2. Generally speaking the impulse is to reduce lower speed cost, more secrecy, and greater robustness are features that distinguish impulsive control. When the continuous delayed neural network is exponentially stable but the impulses are input disturbances, sufficient conditions for exponential stability concerned with the magnitude and frequency of impulses are derived to maintain the exponential stability of the original neural network. When the continuous neural network is unstable, sufficient stability conditions that utilize impulsive effects to stabilize the unstable neural network are given. For example, [9,33] investigates the impulsive synchronization of neural networks. The authors of [53] examined the stability of a type of inertial BAM neural networks with delays that are time-varying. In particular, in [9], impulsive control was used to examine the dynamical and static multi synchronization issues. In order to achieve the desired control performance, we can design the impulsive strength artificially. Since actuator saturation is a common occurrence in almost all control systems, it is actually very challenging from the perspective of applications to accomplish the design aim for each control input. Moreover, in the aforementioned studies, the saturation structure of impulses has been neglected. Despite the fact that the synchronization problem has been analyzed by various researchers for neural networks that have saturated impulsive control in recent years [18,43,46], there are still certain issues to investigate. This paper provides insights on impulse action, particularly the saturation structure and proposes a novel method for evaluating the synchronization of neural networks with inertial term and coupling delay.

In the following the effective control scheme $\nu_1(t), \nu_2(t)$ in (6) is provided by the actuator situation, i.e $\nu_1(t) = \sum_{k=0}^{\infty} sat(\vartheta_1(t))\delta(t-t_k), \nu_2(t) = \sum_{k=0}^{\infty} sat(\vartheta_2(t))\delta(t-t_k), \mathbb{M} \le t_{k+1} - t_k \le M, k \in \mathbb{Z}_+$ where $\mathbb{M}$ and M are positive constants. Different from previous theorems we are going to consider the actuator situation asymmetric character. Let $\vartheta_1(t) = \bar{\mathfrak{K}}_1 e_1(t), \vartheta_2(t) = \bar{\mathfrak{K}}_2 e_2(t)$, where $\bar{\mathfrak{K}}_1, \bar{\mathfrak{K}}_2$ are control gains. When $i = 1, 2, \cdots n$, each component $sat(\bar{\mathfrak{K}}_{1i} e_1(t)), sat(\bar{\mathfrak{K}}_{2i} e_2(t))$ is therefore denoted as

$$sat(\bar{\mathfrak{K}}_{1i} e_1(t)) = \begin{cases} -\chi_i, & \bar{\mathfrak{K}}_{1i} e_1(t) < -\chi_i \\ \bar{\mathfrak{K}}_{1i} e_1(t), & \bar{\mathfrak{K}}_{1i} e_1(t) \in [-\chi_i, \eta_i], \\ \eta_i, & \bar{\mathfrak{K}}_{1i} e_1(t) > \eta_i \end{cases} sat(\bar{\mathfrak{K}}_{2i} e_2(t)) = \begin{cases} -\chi_i, & \bar{\mathfrak{K}}_{2i} e_2(t) < -\chi_i \\ \bar{\mathfrak{K}}_{2i} e_2(t), & \bar{\mathfrak{K}}_{2i} e_2(t) \in [-\chi_i, \eta_i], \\ \eta_i, & \bar{\mathfrak{K}}_{2i} e_2(t) > \eta_i \end{cases}$$

where $\eta_i, \chi_i > 0$. The following formula can then be used straight away [11]:

$$sat^s\big(\bar{\mathfrak{K}}_{1i} e_1(t) - \tilde{\xi}_i\big) = \begin{cases} \bar{\xi}_i, & \bar{\mathfrak{K}}_{1i} e_1(t) - \tilde{\xi}_i > \bar{\xi}_i \\ \bar{\mathfrak{K}}_{1i} e_1(t) - \tilde{\xi}_i, & -\bar{\xi}_i \le \bar{\mathfrak{K}}_{1i} e_1(t) - \tilde{\xi}_i \le \bar{\xi}_i, \\ -\bar{\xi}_i, & \bar{\mathfrak{K}}_{1i} e_1(t) - \tilde{\xi}_i < -\bar{\xi}_i \end{cases}$$

$$sat^s\big(\bar{\mathfrak{K}}_{2i} e_2(t) - \tilde{\xi}_i\big) = \begin{cases} \bar{\xi}_i, & \bar{\mathfrak{K}}_{2i} e_2(t) - \tilde{\xi}_i > \bar{\xi}_i \\ \bar{\mathfrak{K}}_{2i} e_2(t) - \tilde{\xi}_i, & -\bar{\xi}_i \le \bar{\mathfrak{K}}_{2i} e_2(t) - \tilde{\xi}_i \le \bar{\xi}_i, \\ -\bar{\xi}_i, & \bar{\mathfrak{K}}_{2i} e_2(t) - \tilde{\xi}_i < -\bar{\xi}_i \end{cases}$$

where $\bar{\xi}_i = \frac{\eta_i + \chi_i}{2}, \tilde{\xi}_i = \frac{\eta_i - \chi_i}{2}$. Clearly, $sat^s\big(\bar{\mathfrak{K}}_{1i} e_1(t) - \tilde{\xi}_i\big)$ and $sat^s\big(\bar{\mathfrak{K}}_{2i} e_2(t) - \tilde{\xi}_i\big)$ are two symmetrical non normalized saturation functions respectively. The asymmetric saturation functions can therefore be stated as:

$$sat(\mathfrak{K}_1 e_1(t)) = sat^s(\mathfrak{K}_1 e_1(t) - \tilde{\xi}) + \tilde{\xi}, sat(\mathfrak{K}_2 e_2(t)) = sat^s(\mathfrak{K}_2 e_2(t) - \tilde{\xi}) + \tilde{\xi}, \tag{20}$$

where $\eta = (\eta_1, \eta_2, \ldots, \eta_n)^T, \chi = (\chi_1, \chi_2, \ldots, \chi_n)^T$ and $\tilde{\xi} = \frac{\eta - \chi}{2}$. Thereafter, we rewrite the error system in the following manner:

$$\begin{cases} \frac{de_1(t)}{dt} = & -e_1(t) + e_2(t), \\ \frac{de_2(t)}{dt} = & \mathfrak{A} e_1(t) - \mathfrak{B} e_2(t) + \hat{C} f(e_1(t)) + \hat{D} f(e_1(t - \varphi(t))) + I(t) + \sum_{j=1}^{N} \mathscr{H}_{ij} \mathscr{W} e_1(t) + \sum_{j=1}^{N} \mathscr{H}_{ij} \bar{\mathscr{W}} e_1(t - \sigma(t)), \\ e_1(t_k^+) = & e_1(t_k) + sat(\mathfrak{K}_1 e_1(t_k) - \tilde{\xi}) + \tilde{\xi}, e_2(t_k^+) = e_2(t_k) + sat(\mathfrak{K}_2 e_2(t_k) - \tilde{\xi}) + \xi, t = t_k, \\ e_1(s) = & \xi_1(s), e_2(s) = \xi_2(s), s \in [t_0 - h, t_0]. \end{cases} \tag{21}$$

Using the asymmetric saturated impulsive control technique, we will present some suitable criteria for the synchronization of inertial neural networks in the following theorem. The dead zone function is considered as $dz(\mathfrak{K}_1 e_1(t) - \tilde{\xi})$ and $dz(\mathfrak{K}_2 e_2(t) - \tilde{\xi})$ described by $dz(\mathfrak{K}_1 e_1(t) - \tilde{\xi}) = sat^s(\mathfrak{K}_1 e_1(t) - \tilde{\xi}) - \mathfrak{K}_1 e_1(t) + \tilde{\xi}, dz(\mathfrak{K}_2 e_2(t) - \tilde{\xi}) = sat^s(\mathfrak{K}_2 e_2(t) - \tilde{\xi}) - \mathfrak{K}_2 e_2(t) + \tilde{\xi}$. The error dynamics (21) can therefore be stated as:

$$\begin{cases} \frac{de_1(t)}{dt} = & -e_1(t) + e_2(t), \\ \frac{de_2(t)}{dt} = & \mathfrak{A} e_1(t) - \mathfrak{B} e_2(t) + \hat{C} f(e_1(t)) + \hat{D} f(e_1(t - \varphi(t))) + I(t) + \sum_{j=1}^{N} \mathscr{H}_{ij} \mathscr{W} e_1(t) + \sum_{j=1}^{N} \mathscr{H}_{ij} \bar{\mathscr{W}} e_1(t - \sigma(t)), \\ e_1(t_k^+) = e_1(t_k) + dz(\mathfrak{K}_1 e_1(t) - \tilde{\xi}) + \mathfrak{K}_1 e_1(t_k), & e_2(t_k^+) = e_2(t_k) + dz(\mathfrak{K}_2 e_2(t) - \tilde{\xi}) + \mathfrak{K}_2 e_2(t_k), t = t_k, \\ e_1(s) = & \xi_1(s), e_2(s) = \xi_2(s), s \in [t_0 - h, t_0]. \end{cases} \tag{22}$$

Definition 3.3. The INN system (22) is said to be stable exponentially, if there exists constants $Q \geq 1$ and ϵ, for all initial value $\psi(t)$ such that $|e(t)| \leq Q|\psi(t)|\exp(-\epsilon(t-t_0)), t \geq t_0$, is in a domain Υ that includes the origin's open section. Suppose $\Upsilon = R^n$, it is said to be globally stable.

Theorem 3.4. *Suppose that there exist constants* $\alpha_1 > 0, \alpha_2 > 0, \alpha_3 > 0, \alpha_4 > 0$ *and some* $n \times n$ *diagonal matrices* $P_1 > 0, P_2 > 0, M > 0, Z_1 > 0, Z_2 > 0, M^T Z_2 M \leq 0$ *and matrices* $U, W > 0$ *such that the following inequalities hold:*

$$I_N \otimes \left(2P_1 - P_1 M + M^T Z_1 M + P_2 \mathfrak{A}\delta^{-1} + (\mathscr{H} \otimes P_2 \mathscr{W})\varsigma^{-1} - \alpha_1 P_1\right) \leq 0, \tag{23}$$

$$I_N \otimes \left(P_1 M^{-1} + P_2 \mathfrak{A}\delta - 2P_2 \mathfrak{B} + P_2 \hat{C} Z_1^{-1} \hat{C}^T P_2 + P_2 \hat{D} Z_2^{-1} \hat{D}^T P_2 + (\mathscr{H} \otimes P_2 \mathscr{W})\varsigma + \left(\mathscr{H}\mathscr{H}^T \otimes P_2 \bar{\mathscr{W}} Z_3^{-1} \bar{\mathscr{W}} P_2\right) - \alpha_1 P_2\right) \leq 0, \tag{24}$$

$$\begin{bmatrix} (I+\mathfrak{K}_1)^T P_1 (I+\mathfrak{K}_1) - \tilde{\Delta}_1 P_1 & (I+\mathfrak{K}_1)^T P_1 - \frac{1}{2} U^T W \\ & P_1 - W \end{bmatrix} \leq 0, \tag{25}$$

$$\begin{bmatrix} (I+\mathfrak{K}_1)^T P_2 (I+\mathfrak{K}_1) - \tilde{\Delta}_2 P_2 & (I+\mathfrak{K}_1)^T P_2 - \frac{1}{2} U^T W \\ & P_2 - W \end{bmatrix} \leq 0, \tag{26}$$

$$\ln \tilde{\Delta} + \alpha_1 T < 0, \tag{27}$$

then the leader-following synchronization between INN (1) and (3) will be realized.

Proof: A Lyapunov functional candidate is constructed as follows

$$\mathscr{V}(t) = \mathscr{V}_1(t) + \mathscr{V}_2(t), \tag{28}$$

where $\mathscr{V}_1(t) = \sum_{i=1}^{N} e_{1i}^T(t) P_1 e_{1i}(t)$, $\mathscr{V}_2(t) = \sum_{i=1}^{N} e_{2i}^T(t) P_2 e_{2i}(t)$.

Taking the derivative of $\mathscr{V}(t)$ along the trajectories of (6)

$$\begin{aligned} D^+\mathscr{V}_1(t) =& 2\sum_{i=1}^{N} e_{1i}^T(t) P_1 \dot{e}_{1i}(t), \\ =& -2\sum_{i=1}^{N} e_{1i}^T(t) P_1 e_{1i}(t) + 2\sum_{i=1}^{N} e_{1i}^T(t) P_1 e_{2i}(t), \\ \leq& -2\sum_{i=1}^{N} P_1 e_{1i}^T(t) e_{1i}(t) + \sum_{i=1}^{N} P_1 e_{1i}^T(t) M e_{1i}(t) + \sum_{i=1}^{N} P_1 e_{2i}^T(t) M^{-1} e_{2i}(t), \end{aligned}$$

$$\begin{aligned} D^+\mathscr{V}_2(t) =& 2\sum_{i=1}^{N} e_{2i}^T(t) P_2 \dot{e}_{2i}(t), \\ =& 2\sum_{i=1}^{N} e_{2i}^T(t) P_2 \Bigg(\mathfrak{A} e_{1i}(t) - \mathfrak{B} e_{2i}(t) + \hat{C} f(e_{1i}(t)) + \hat{D} f(e_{1i}(t-\varphi(t))) + I(t) + \sum_{j=1}^{N} \mathscr{H}_{ij} \mathscr{W} e_{1i}(t) \\ &+ \sum_{j=1}^{N} \mathscr{H}_{ij} \bar{\mathscr{W}} e_{1i}(t-\sigma(t)) \Bigg), \\ =& 2\sum_{i=1}^{N} e_{2i}^T(t) P_2 \mathfrak{A} e_{1i}(t) - 2\sum_{i=1}^{N} e_{2i}^T(t) P_2 \mathfrak{B} e_{2i}(t) + 2\sum_{i=1}^{N} e_{2i}^T(t) P_2 \hat{C} f(e_{1i}(t)) + 2\sum_{i=1}^{N} e_{2i}^T(t) P_2 \hat{D} f(e_{1i}(t-\varphi(t))) \\ &+ 2\sum_{i=1}^{N} e_{2i}^T(t) P_2 \sum_{j=1}^{N} \mathscr{H}_{ij} \mathscr{W} e_{1i}(t) + 2 e_{2i}^T(t) P_2 \sum_{j=1}^{N} \mathscr{H}_{ij} \bar{\mathscr{W}} e_{1i}(t-\sigma(t)). \end{aligned}$$

Then, we can get

$$\begin{aligned} D^+\mathscr{V}(t) =& 2\sum_{i=1}^{N} P_1 e_{1i}^T(t) e_{1i}(t) - \sum_{i=1}^{N} P_1 M e_{1i}^T(t) e_{1i}(t) + \sum_{i=1}^{N} P_1 M^{-1} e_{2i}^T(t) e_{2i}(t) + \sum_{i=1}^{N} P_2 \mathfrak{A}\delta e_{2i}^T(t) e_{2i}(t) \\ &+ \sum_{i=1}^{N} P_2 \mathfrak{A}\delta^{-1} e_{1i}^T(t) e_{1i}(t) - 2\sum_{i=1}^{N} P_2 \mathfrak{B} e_{2i}^T(t) e_{2i}(t) + \sum_{i=1}^{N} e_{2i}^T(t) P_2 \hat{C} Z_1^{-1} \hat{C}^T P_2 e_{2i}(t) + \sum_{i=1}^{N} e_{1i}^T(t) M^T Z_1 M e_{1i}(t) \end{aligned}$$

$$
\begin{aligned}
&+\sum_{i=1}^{N} e_{2i}^T(t)P_2\hat{D}Z_2^{-1}\hat{D}^TP_2e_{2i}(t)+\sum_{i=1}^{N} e_{1i}^T(t-\varphi(t))M^TZ_2Me_{1i}(t-\varphi(t))+e_2^T(\mathscr{H}\otimes P_2\mathscr{W})\varsigma(t)e_2(t)\\
&+e_1^T(t)(\mathscr{H}\otimes P_2\mathscr{W})\varsigma^{-1}e_1(t)+e_2^T(t)\left(\mathscr{H}\mathscr{H}^T\otimes P_2\bar{\mathscr{W}}Z_3^{-1}\bar{\mathscr{W}}P_2\right)e_2(t)+e_1^T(t-\sigma(t))(I_N\otimes Z_3)e_1(t-\sigma(t)),\\
\le& e_1^T(t)\left[I_N\otimes\left(2P_1-P_1M+M^TZ_1M+P_2\mathfrak{A}\delta^{-1}+(\mathscr{H}\otimes P_2\mathscr{W})\varsigma^{-1}-\alpha_1P_1\right)\right]e_1(t)\\
&+e_2^T(t)\left[I_N\otimes\left(P_1M^{-1}+P_2\mathfrak{A}\delta-2P_2\mathfrak{B}+P_2\hat{C}Z_1^{-1}\hat{C}^TP_2+P_2\hat{D}Z_2^{-1}\hat{D}^TP_2+(\mathscr{H}\otimes P_2\mathscr{W})\varsigma\right.\right.\\
&+\left.\left.\left(\mathscr{H}\mathscr{H}^T\otimes P_2\bar{\mathscr{W}}Z_3^{-1}\bar{\mathscr{W}}P_2\right)-\alpha_1P_2\right)\right]e_2(t)\\
&+e_1^T(t-\varphi(t))\left[I_N\otimes\left(M^TZ_2M\right)\right]e_1(t-\varphi(t))\\
&+e_1^T(t-\sigma(t))[I_N\otimes Z_3]e_1(t-\sigma(t))+e_1^T(t)\alpha_1P_1e_1(t)+e_2^T(t)\alpha_1P_2e_2(t),\\
\le&\alpha_1\mathscr{V}(t).
\end{aligned}\tag{29}
$$

From Lemma 2.7, if $e_1(t), e_2(t)\in\mathbb{U}$, where set $\mathbb{U}=\left\{e_1(t),e_2(t)\in\mathbb{R}^n : -\hat{\delta}_i\le\mathfrak{K}_{i1}e_1(t)-\tilde{\xi}_i-U_ie_1(t)\le\hat{\delta}_i, i=1,2,\cdots N\right\}$, $\hat{\delta}=\frac{\eta+\chi}{2}$, we can get $-dz^T(\mathfrak{K}_1e_1(t)-\tilde{\xi})W(dz(\mathfrak{K}_1e_1(t)-\tilde{\xi})+Ue_1(t))\ge 0$, $-dz^T(\mathfrak{K}_1e_2(t)-\tilde{\xi})W(dz(\mathfrak{K}_1e_2(t)-\tilde{\xi})+Ue_2(t))\ge 0$, i.e, if $e_1(t), e_2(t)\in\mathbb{U}$, where set $\mathbb{U}=\{e_1(t),e_2(t)\in\mathbb{R}^n : -\chi_i\le\mathfrak{K}_{i1}e_1(t)-U_ie_1(t)\le\eta_i, i=1,2,\cdots N\}$, then

$$
-dz^T(\mathfrak{K}_1e_1(t)-\tilde{\xi})W(dz(\mathfrak{K}_1e_1(t)-\tilde{\xi})+Ue_1(t))\ge 0,\ -dz^T(\mathfrak{K}_1e_2(t)-\tilde{\xi})W(dz(\mathfrak{K}_1e_2(t)-\tilde{\xi})+Ue_2(t))\ge 0 \tag{30}
$$

Taking $\tilde{\mathbb{U}}=\{e_1(t),e_2(t)\in\mathbb{R}^n : -\min(\eta_i,\chi_i)\le\mathfrak{K}_{i1}e_1(t)-U_ie_1(t)\le\min(\eta_i,\chi_i), i=1,2,\cdots N\}$, one obtains $\tilde{\mathbb{U}}\subseteq\mathbb{U}$. When $t=t_0$, from (30), one obtains

$$
\begin{aligned}
&-dz^T(\mathfrak{K}_1e_1(t_0)-\tilde{\xi})W(dz(\mathfrak{K}_1e_1(t_0)-\tilde{\xi})+Ue_1(t_0))\ge 0,\\
&-dz^T(\mathfrak{K}_1e_2(t_0)-\tilde{\xi})W(dz(\mathfrak{K}_1e_2(t_0)-\tilde{\xi})+Ue_2(t_0))\ge 0.
\end{aligned}\tag{31}
$$

And one can demonstrate this

$$
\begin{aligned}
\mathscr{V}\left(t_0^+\right)=&\left(e_1(t_0)+dz\left(\mathfrak{K}_1e_1(t_0)-\tilde{\xi}\right)+\mathfrak{K}_1e_1(t_0)\right)^TP_1\left(e_1(t_0)+dz\left(\mathfrak{K}_1e_1(t_0)-\tilde{\xi}\right)+\mathfrak{K}_1e_1(t_0)\right)\\
&+\left(e_2(t_0)+dz\left(\mathfrak{K}_1e_2(t_0)-\tilde{\xi}\right)+\mathfrak{K}_1e_2(t_0)\right)^TP_2\left(e_2(t_0)+dz\left(\mathfrak{K}_1e_2(t_0)-\tilde{\xi}\right)+\mathfrak{K}_1e_2(t_0)\right),\\
\le& e_1(t_0)^T(I+\mathfrak{K}_1)^TP_1(I+\mathfrak{K}_1)e_1(t_0)+e_1(t_0)^T(I+\mathfrak{K}_1)^TP_1dz\left(\mathfrak{K}_1e_1(t_0)-\tilde{\xi}\right)\\
&+dz^T\left(\mathfrak{K}_1e_1(t_0)-\tilde{\xi}\right)P_1(I+\mathfrak{K}_1)e_1(t_0)+dz^T\left(\mathfrak{K}_1e_1(t_0)-\tilde{\xi}\right)P_1dz\left(\mathfrak{K}_1e_1(t_0)-\tilde{\xi}\right)\\
&+e_2(t_0)^T(I+\mathfrak{K}_1)^TP_2(I+\mathfrak{K}_1)e_2(t_0)+e_2(t_0)^T(I+\mathfrak{K}_1)^TP_2dz\left(\mathfrak{K}_1e_2(t_0)-\tilde{\xi}\right)\\
&+dz^T\left(\mathfrak{K}_1e_2(t_0)-\tilde{\xi}\right)P_2(I+\mathfrak{K}_1)e_2(t_0)+dz^T\left(\mathfrak{K}_1e_2(t_0)-\tilde{\xi}\right)P_2dz\left(\mathfrak{K}_1e_2(t_0)-\tilde{\xi}\right)\\
&-dz^T\left(\mathfrak{K}e_1(t_0)-\tilde{\xi}\right)Wdz\left(\mathfrak{K}e_1(t_0)-\tilde{\xi}\right)-dz^T\left(\mathfrak{K}e_1(t_0)-\tilde{\xi}\right)WUe_1(t_0)\\
&-dz^T\left(\mathfrak{K}e_2(t_0)-\tilde{\xi}\right)Wdz\left(\mathfrak{K}_1e_2(t_0)-\tilde{\xi}\right)-dz^T\left(\mathfrak{K}_1e_2(t_0)-\tilde{\xi}\right)WUe_2(t_0)\\
&-\tilde{\Delta}_1e_1(t_0)^TP_1e_1(t_0)+\tilde{\Delta}_1e_1(t_0)^TP_1e_1(t_0)-\tilde{\Delta}_2e_2(t_0)^TP_2e_2(t_0)+\tilde{\Delta}_2e_2(t_0)^TP_2e_2(t_0),\\
\le&\tilde{\Delta}\mathscr{V}(t_0).
\end{aligned}\tag{32}
$$

From (29) and (32), one can get that when $k=0, t_0<t\le t_1$,

$$
\begin{aligned}
\mathscr{V}(t)\le&\mathscr{V}(t_0^+)\exp(\alpha_1(t-t_0)),\\
\le&\tilde{\Delta}\mathscr{V}(t_0)\exp(\alpha_1(t-t_0)),\\
\mathscr{V}(t_1)\le&\tilde{\Delta}\mathscr{V}(t_0)\exp(\alpha_1(t_1-t_0)).
\end{aligned}\tag{33}
$$

Therefore, it is easy to see that $\mathscr{V}(t_1)\le\mathscr{V}(t_0)\exp(\ln\tilde{\Delta}+\alpha_1T)$. And from condition (27), $In\tilde{\Delta}+\alpha_1T<0$, we get $\mathscr{V}(t_1)\le\theta$, i.e $e_1(t_1)^TP_1e_1(t_1)+e_2(t_1)^TP_2e_2(t_1)\le\theta$, that is $e_1(t_1), e_2(t_1)\subset\mathbb{U}$. Similarly, we get

$$
\begin{aligned}
\mathscr{V}\left(t_1^+\right)\le&\tilde{\Delta}\mathscr{V}(t_1),\\
\le&\tilde{\Delta}^2\mathscr{V}(t_0)\exp(\alpha_1(t_1-t_0)).
\end{aligned}\tag{34}
$$

When $k=1, t_1<t\le t_2$, we get

$$
\begin{aligned}
\mathscr{V}(t)\le&\mathscr{V}e\left(t_1^+\right)\exp(\alpha_1(t-t_1)),\\
\le&\tilde{\Delta}^2\mathscr{V}(t_0)\exp(\alpha_1(t-t_0)),\\
\mathscr{V}(t_2)\le&\tilde{\Delta}^2\mathscr{V}(t_0)\exp(\alpha_1(t_2-t_0)).
\end{aligned}\tag{35}
$$

By means of mathematical deduction, when $k = h - 1, t_{h-1} < t \le t_h$, suppose that

$$\mathscr{V}(t) \le \tilde{\Delta}^h \mathscr{V}(t_0) \exp(\alpha_1(t - t_0)),$$
$$\mathscr{V}(t_k) \le \tilde{N}^h \mathscr{V}(t_0) \exp(\alpha_1(t_k - t_0)). \tag{36}$$

It is simple to demonstrate that $\mathscr{V}(t_k) \le \mathscr{V}(t_0)\exp(h(\ln\tilde{\Delta} + \alpha_1 T))$. From (27), one can get $\mathscr{V}(t_k) \le \theta$, i.e $e_1^T(t_k)P_1 e_1(t_k) + e_2^T(t_k)P_2 e_2(t_k) \le \theta$. Therefore, $e_1(t_k), e_2(t_k) \subset \mathbb{U}$. And from (30), one has

$$\mathscr{V}\left(t_k^+\right) \le \tilde{\Delta}\mathscr{V}(t_k) \le \tilde{\Delta}^{h+1}\mathscr{V}(t_0)\exp(\alpha_1(t_k - t_0)). \tag{37}$$

When $k = h, t_h < t \le t_{h+1}$, we obtain,

$$\mathscr{V}(e(t)) \le \tilde{\Delta}^{k+1}\mathscr{V}(e(t_0))\exp(\mu(t - t_0)),$$
$$\le \mathscr{V}(e(t_0))\exp((k+1)(\ln\tilde{N} + \mu T)). \tag{38}$$

Suppose that for $t_h < t \le t_{h+1}$, one derives that $t - t_0 \le t_{h+1} - t_0 = t_{h+1} - t_h + t_h + \cdots - t_1 + t_1 - t_0 \le (h+1)T$. Hence, $\frac{t-t_0}{T} \le h+1$. From the theorem condition (27), $In\tilde{\Delta} + \alpha_1 T < 0$, it is simple to demonstrate this, when $t_h < t \le t_{h+1}$,

$$\mathscr{V}(t) \le \mathscr{V}(t_0)\exp\left(\frac{t - t_0}{T}(ln\tilde{\Delta} + \alpha_1 T)\right) \tag{39}$$

and

$$\mathscr{V}(t) \le \mathscr{V}(t_0)\exp\left(-(t - t_0)\left(-\frac{\ln\tilde{\Delta}}{T} - \alpha_1\right)\right). \tag{40}$$

Therefore from (28)

$$\lambda_{\min}(P)||e(t)||^2 \le \mathscr{V}(t) \le \lambda_{\max}(P)||e(t)||^2, \tag{41}$$

where $e(t) = (e_1(t), e_2(t))^T, P = diag(P_1, P_2)$, then the inequality provided below holds true:

$$||e(t)|| \le \sqrt{\frac{\mathscr{V}(e(t_0))}{\lambda_{\min}(P)}}\exp\left(-(t - t_0)\frac{1}{2}\left(-\frac{1}{T}\ln\tilde{\Delta} - \alpha_1\right)\right). \tag{42}$$

Therefore, from Definition 3.3, and conditions (23) – (27), every trajectory of the error signal converge to the origin as $t \to \infty$, for all $t \ge t_0$. That is, the leader-following synchronization between addressed leader-follower systems through the control law (20) will be achieved.

4. Numerical simulations

This section includes two examples to further illustrate our results.

Example 4.1. Consider the INN (1) with coupling delays and the isolated node (3) with the corresponding system parameters: $\Gamma = 3, n = 2, I(t) = (0,0)^T, \varphi(t) = 1, \sigma(t) = 1, f_i(\omega_i(t)) = \tanh(\omega_i(t)), i = 1,2,3,4,5$ and matrices $\hat{A}, \hat{B}, \hat{C}, \hat{D}$ are given by:

$$\hat{A} = \begin{pmatrix} 1 & 0 \\ 0 & 1 \end{pmatrix}, \hat{B} = \begin{pmatrix} 1 & 0 \\ 0 & 1 \end{pmatrix}, \hat{C} = \begin{pmatrix} \frac{\pi}{4} + 1 & 20.01 \\ 0.12 & \frac{\pi}{4} + 1 \end{pmatrix}, \hat{D} = \begin{pmatrix} -\pi\frac{1.3}{2\sqrt{2}} & 0.11 \\ 0.11 & -\pi\frac{1.3}{2\sqrt{2}} \end{pmatrix}.$$

The delayed and non-delayed coupling matrices $\bar{\mathscr{W}}$ and $\mathscr{W}$ are given as follows:

$$\bar{\mathscr{W}} = \begin{pmatrix} 0.4 & 0 \\ 0 & 0.4 \end{pmatrix}, \quad \mathscr{W} = \begin{pmatrix} 0.2 & 0 \\ 0 & 0.2 \end{pmatrix}.$$

Fig. 1, shows the coupled network's topological structure. The following is the equivalent Laplacian matrix and leader adjacency matrix:

$$L = \begin{pmatrix} 1 & 0 & 0 & -1 & 0 \\ -1 & 1 & 0 & 0 & 0 \\ 0 & -1 & 1 & 0 & 0 \\ 0 & 0 & -1 & 1 & 0 \\ 0 & -1 & 0 & 0 & 1 \end{pmatrix},$$
$$H = \mathrm{diag}\{1, 0, 1, 0, 0\}.$$

The phase diagram of the node that is isolated (4) with the initial values $h(0) = (1.0, 2.01)T, y(0) = (1.0, 2.01)T$ is shown in Fig. 2. When there is no control input, the coupled delayed INN(1) cannot achieve the same synchronization behavior as the isolated inertial delayed neural networks (3). The coupled delayed INN (1) will be synchronized exponentially to the

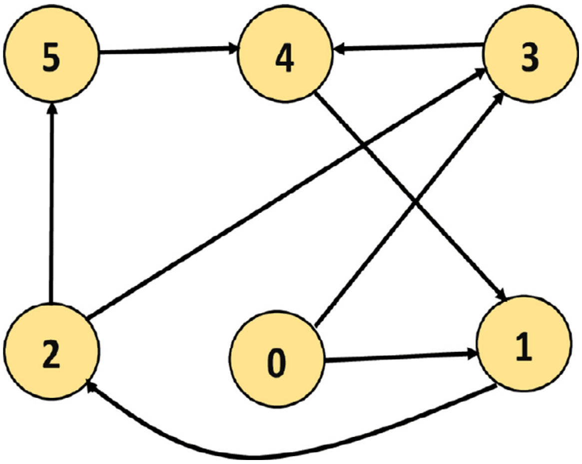

Fig. 1. The topological structure of the network.

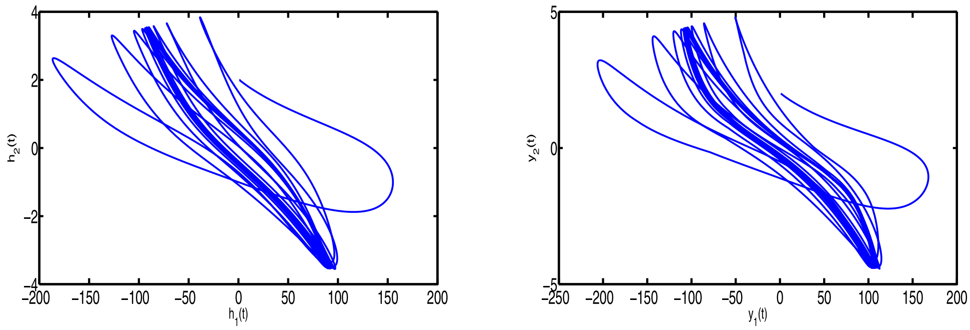

Fig. 2. The phase plot of the isolated node (4).

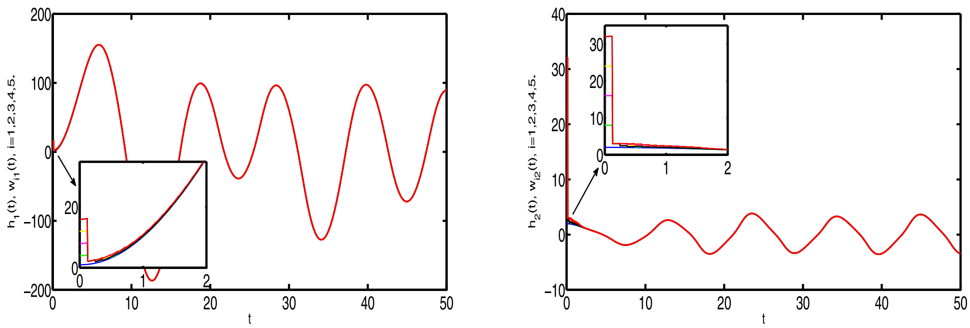

Fig. 3. The state trajectories with saturated impulsive control.

isolated node (3). The saturation control with impulses will be developed as follows. To that aim, we examine the saturation level $S_i = (1, 1)^T, \ i = 1, 2, 3, 4, 5$ while also obtaining certain matrices as follows:

$$P_1 = \begin{pmatrix} 0.04 & 0 \\ 0 & 0.04 \end{pmatrix}, \quad P_2 = \begin{pmatrix} 0.102 & 0 \\ 0 & 0.102 \end{pmatrix}. \tag{43}$$

The leader following error system (6), according to Theorem 3.1, converges to zero exponentially when the impulsive sequence is $t_{2n} = 0.12n, \ n \in \mathbb{Z}_+$. Synchronization between INNs with coupling delays (1) and neural network node with inertial term and isolated delay (3) is achieved via the impulsive saturated control as exhibited in the Figs. 3,4,5.

Remark 4.1. Because equation (1) with the parameters in Example 4.1 is initially unstable, most known studies on the synchronization problem of delayed inertial neural networks without impulses like [2,34,38] cannot be applied to it. On the contrary, the saturated impulsive control approaches suggested in this study can successfully achieve exponential synchronization.

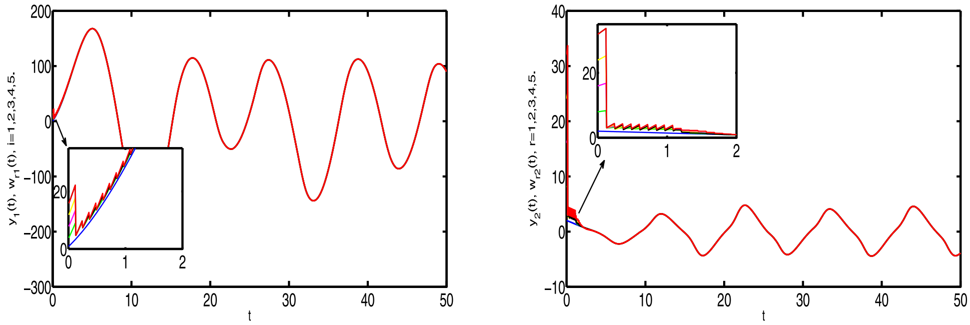

Fig. 4. The state trajectories with saturated impulsive control.

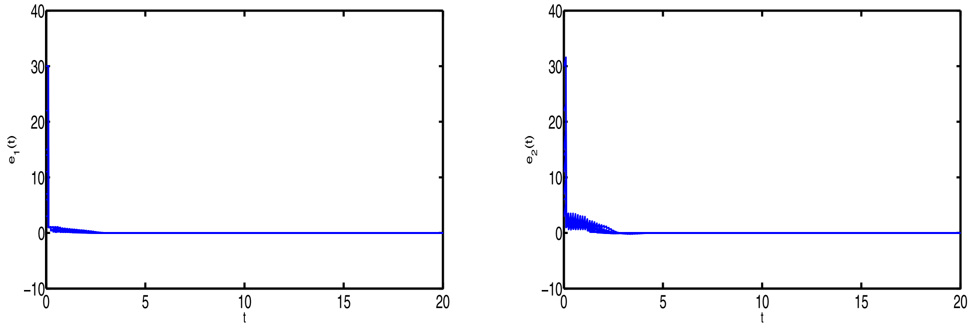

Fig. 5. The error signals with saturated impulsive control.

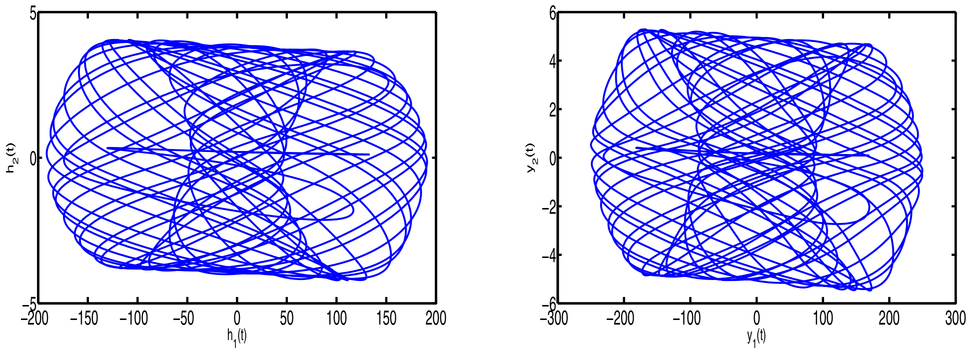

Fig. 6. The chaotic behavior of the isolated node (4) in Example 4.2.

Example 4.2. Consider the underlying coupled delayed INNs which take into account both current-state and delayed coupling:

$$\frac{d^2\omega_i(t)}{dt^2} = -\hat{A}\frac{d\omega_i(t)}{dt} - \hat{B}\omega_i(t) + \hat{C}f(\omega_i(t)) + \hat{D}f(\omega_i(t-\varphi(t))) + I(t) + \sum_{j=1}^{N}\mathscr{H}_{ij}\mathscr{W}\omega_j(t) + \sum_{j=1}^{N}\mathscr{H}_{ij}\bar{\mathscr{W}}\omega_j(t-\sigma(t)), \tag{44}$$

where the values of $\hat{A}, \hat{B}, \hat{C}, \hat{D}, \mathscr{W}$ and $\bar{\mathscr{W}}$ are given as follows:

$$\hat{A} = \begin{pmatrix} 0.4 & 0 \\ 0 & 0.4 \end{pmatrix}, \quad \hat{B} = \begin{pmatrix} 1.6 & 0 \\ 0 & 1.6 \end{pmatrix}, \quad \hat{C} = \begin{pmatrix} 1.8 & 18 \\ 0.2 & 1.8 \end{pmatrix}, \quad \hat{D} = \begin{pmatrix} -2 & 0.1 \\ 0 & -2 \end{pmatrix},$$

$$\mathscr{W} = \begin{pmatrix} 0.6 & 0. \\ 0 & 0.6 \end{pmatrix}, \quad \bar{\mathscr{W}} = \begin{pmatrix} 0.4 & 0 \\ 0 & 0.4 \end{pmatrix},$$

and $f(\omega_i(t)) = (|\omega_i(t)+1| - |\omega_i(t)-1|)/2, \varphi = 1, \sigma = 1, i = 1,2,3,4,5$, then inertial neural networks (1) exists chaotic behavior with the initial values $h(0) = (0.1, 0.2)^T$ which is shown in Fig. 6. Now examine the INNs with exponential synchronization (44) and asymmetric saturated impulsive control (20). If $\eta = 0.1$, we can deduce that the coupled delayed inertial

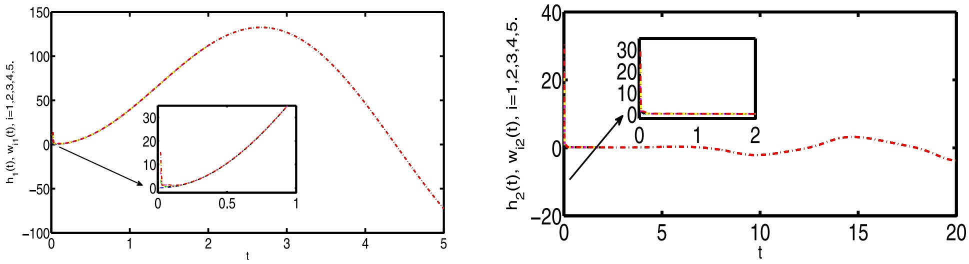

Fig. 7. The state trajectories with asymmetric saturated impulsive control.

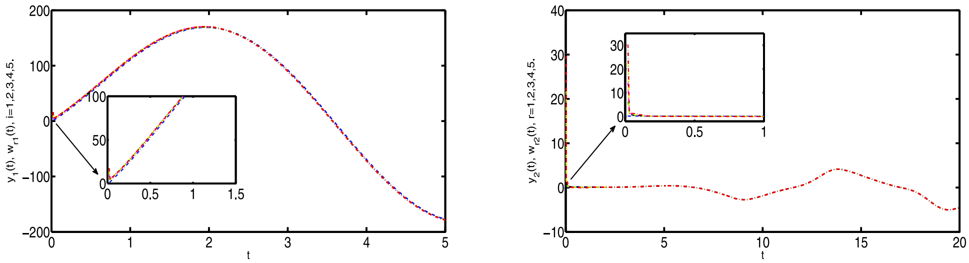

Fig. 8. The state trajectories with asymmetric saturated impulsive control.

neural networks (44) are exponentially synchronized with the isolated node (3) under asymmetric saturated impulsive control (20) using Theorem 3.2. Figs. 7 and 8 demonstrate the state trajectories of inertial neural networks (44) under the initial conditions $\xi_i(s) = (3i, 6i)^T, \bar{\xi}_i(s) = (3i, 6i)^T,\ i = 1, 2, 3, 4, 5.$

Remark 4.2. Actuator saturation nonlinearities are common in many dynamical systems because every physical actuator is subject to its maximum and minimum limits. Impulse saturation may be detrimental to the synchronization process as compared to unconstrained impulsive control. Figs. 3 and 4 make it clear that the impulsive controller's saturation reduces the rate at which synchronization convergence occurs. That is because the actuator saturation degrades the performance of the system. The asymmetric character of saturation is very common in practical situations. It is easy to see from Fig. 7 and 8 that the existence of asymmetric saturation in the impulsive controller further slows down the convergence rate than the actuator saturation of the synchronization.

5. Conclusion

In this article, some novel suitable conditions for the leader-following synchronization problem of neural networks with inertial term are proposed that considers two types of delays at the same time. Using variable transformation on inertial neural networks, a given model can be transformed into first order differential equations and by substituting saturation non linearity for a dead-zone function and some adequate conditions for the exponential synchronization of coupled delayed INNs can be deduced in terms of LMIs. In addition, an asymmetric saturated impulsive control method is proposed in the leader-following synchronization pattern to achieve exponential synchronization of the addressed INNs. Finally, simulation results are used to validate the theoretical research findings. It should be noted that our findings are only applicable in situations when the impulse and time delay are known or measured. On the other hand, the impulse signal can sometimes be controlled or monitored throughout many application scenarios, particularly in control components, and it is also stochastic. Actuator saturation can be addressed using one of two strategies. The first one takes into account the saturation nonlinearity at the outset of the control design based on a control law, another is referred to as a anti-windup compensator, which adds more feedbacks to the actuator to maintain it within acceptable bounds. The primary benefit of this approach is that the compensator functions in concert with the existing linear controller and only intervenes when saturation is reached. The issue of master-slave fixed-time synchronization of a discontinuous coupled inertial neural network with saturation actuator indefinite functionals will be the focus on future research.

Declaration of competing interest

The authors declare that they have no known competing financial interests or personal relationships that could have appeared to influence the work reported in this paper.

Data Availability

No data was used for the research described in the article.

Acknowledgement

The work of Ardak Kashkynbayev is funded by the Science Committee of the Ministry of Education and Science of the Republic of Kazakhstan Grant OR11466188 ("Dynamical Analysis and Synchronization of Complex Neural Networks with Its Applications") and Nazarbayev University under Collaborative Research Program Grant No 11022021CRP1509.

References

[1] Q. Song, L. Long, Z. Zhao, Y. Liu, F.E. Alsaadi, Stability criteria of quaternion-valued neutral-type delayed neural networks, Neurocomputing 412 (2020) 287–294.
[2] W. Li, X. Gao, R. Li, Stability and synchronization control of inertial neural networks with mixed delays, Appl. Math. Comput. 367 (2020) 124779.
[3] R. Rakkiyappan, E.U. Kumari, A. Chandrasekar, R. Krishnasamy, Synchronization and periodicity of coupled inertial memristive neural networks with supremums, Neurocomputing 214 (2016) 739–749.
[4] S. Zhu, H. Bao, Event-triggered synchronization of coupled memristive neural networks, Appl. Math. Comput. 415 (2022) 126715.
[5] Q. Xiao, H. Liu, Y. Wang, An improved finite-time and fixed-time stable synchronization of coupled discontinuous neural networks, IEEE Trans. Neural. Netw. Learn. Syst. (2021), doi:10.1109/TNNLS.2021.3116320.
[6] L. Feng, C. Hu, J. Yu, H. Jiang, S. Wen, Fixed-time synchronization of coupled memristive complex-valued neural networks, Chaos Soliton. Fractals. 148 (2021) 110993.
[7] Y. Huang, F. Wu, Finite-time passivity and synchronization of coupled complex-valued memristive neural networks, Inf. Sci. 580 (2021) 775–800.
[8] Z. Cai, L. Huang, L. Zhang, Finite-time synchronization of master-slave neural networks with time-delays and discontinuous activations, Appl. Math. Model. 47 (2017) 208–226.
[9] X. Lv, X. Li, J. Cao, M. Perc, Dynamical and static multisynchronization of coupled multistable neural networks via impulsive control, IEEE Trans. Neural Netw. Learn. Syst. 29 (12) (2018) 6062–6072.
[10] C. Huang, Exponential stability of inertial neural networks involving proportional delays and non-reduced order method, J. Exp. Theor. Artif. Intell. 32 (1) (2020) 133–146.
[11] C. Huang, B. Liu, New studies on dynamic analysis of inertial neural networks involving non-reduced order method, Neurocomputing 325 (2019) 283–287.
[12] A. Wu, Y. Chen, S. Zhu, S. Wen, Positivity and stability of cohen-grossberg-type memristor neural networks with unbounded delays, IEEE Trans. Circuits Syst. I: Regul. Pap. 68 (11) (2021) 4508–4519.
[13] A. Kashkynbayev, J. Cao, D. Suragan, Global lagrange stability analysis of retarded SICNNs, Chaos Solit. Fractals 145 (2021) 110819.
[14] S. Jia, C. Hu, J. Yu, H. Jiang, Asymptotical and adaptive synchronization of cohen grossberg neural networks with heterogeneous proportional delays, Neurocomputing 275 (2018) 1449–1455.
[15] X. Li, W. Zhang, J.A. Fang, H. Li, Event-triggered exponential synchronization for complex-valued memristive neural networks with time-varying delays, IEEE Trans. Neural Netw. Learn. Syst. 31 (10) (2019) 4104–4116.
[16] X. Ni, S. Wen, H. Wang, Z. Guo, S. Zhu, T. Huang, Observer-based quasi-synchronization of delayed dynamical networks with parameter mismatch under impulsive effect, IEEE Trans. Neural Netw. Learn. Syst. 32 (7) (2021) 3046–3055.
[17] Z. Wang, L. Huang, Synchronization analysis of linearly coupled delayed neural networks with discontinuous activations, Appl. Math. Model. 39 (23–24) (2015) 7427–7441.
[18] H. Li, C. Li, D. Ouyang, S.K. Nguang, Impulsive synchronization of unbounded delayed inertial neural networks with actuator saturation and sampled–data control and its application to image encryption, IEEE Trans. Neural Netw. Learn. Syst. 32 (4) (2020) 1460–1473.
[19] X. Li, T. Huang, Adaptive synchronization for fuzzy inertial complex-valued neural networks with state-dependent coefficients and mixed delays, Fuzzy Sets Syst. 411 (2021) 174–189.
[20] T. Huang, C. Li, X. Liu, Synchronization of chaotic systems with delay using intermittent linear state feedback, Chaos 18 (3) (2008) 033122.
[21] C.J. Cheng, T.L. Liao, J.J. Yan, C.C. Hwang, Exponential synchronization of a class of neural networks with time-varying delays, IEEE Trans. Syst. Man Cybern. Syst. 36 (1) (2006) 209–215.
[22] G.T. Stamov, I.M. Stamova, Almost periodic solutions for impulsive neural networks with delay, Appl. Math. Model. 31 (7) (2007) 1263–1270.
[23] D. Peng, X. Li, R. Rakkiyappan, Y. Ding, Stabilization of stochastic delayed systems: event-triggered impulsive control, Appl. Math. Comput. 401 (2021) 126054.
[24] Y. Tang, X. Wu, P. Shi, F. Qian, Input-to-state stability for nonlinear systems with stochastic impulses, Automatica 113 (2020) 108766.
[25] S. Wang, Z. Zhang, C. Lin, J. Chen, Fixed-time synchronization for complex-valued BAM neural networks with time-varying delays via pinning control and adaptive pinning control, Chaos Solit. Fractals 153 (2021) 111583.
[26] H. Li, J.A. Fang, X. Li, T. Huang, Exponential synchronization of multiple impulsive discrete-time memristor-based neural networks with stochastic perturbations and time-varying delays, Neurocomputing 392 (2020) 86–97.
[27] F. Tan, L. Zhou, Y. Chu, Y. Li, Fixed-time stochastic outer synchronization in double-layered multi-weighted coupling networks with adaptive chattering-free control, Neurocomputing 399 (2020) 8–17.
[28] T. Yu, H. Wang, M. Su, D. Cao, Distributed-delay-dependent exponential stability of impulsive neural networks with inertial term, Neurocomputing 313 (2018) 220–228.
[29] X. Li, J. Cao, Delay-dependent stability of neural networks of neutral type with time delay in the leakage term, Nonlinearity 23 (7) (2010) 1709.
[30] B. Liu, New convergence behavior of solutions to shunting inhibitory cellular neural networks with unbounded delays and time-varying coefficients, Appl. Math. Model. 33 (1) (2009) 54–60.
[31] L. Wang, K. Zeng, C. Hu, Y. Zhou, Multiple finite-time synchronization of delayed inertial neural networks via a unified control scheme, Knowl Based Syst. 236 (2022) 107785.
[32] M. Tan, Y. Tan, Global exponential stability of periodic solution of neural network with variable coefficients and time-varying delays, Appl. Math. Model. 33 (1) (2009) 373–385.
[33] L. Sheng, H. Yang, Exponential synchronization of a class of neural networks with mixed time-varying delays and impulsive effects, Neurocomputing 71 (16–18) (2008) 3666–3674.
[34] X. Zhong, Y. Gao, Synchronization of inertial neural networks with time-varying delays via quantized sampled-data control, IEEE Trans. Neural Netw. Learn. Syst. 32 (11) (2020) 4916–4930.
[35] X. Li, S. Song, J. Wu, Impulsive control of unstable neural networks with unbounded time-varying delays, Sci. China Inf. Sci. 61 (1) (2018) 1–14.

[36] M.S. Ali, M. Usha, Z. Orman, S. Arik, Improved result on state estimation for complex dynamical networks with time varying delays and stochastic sampling via sampled-data control, Neural Netw. 114 (2019) 28–37.
[37] X. Li, W. Zhang, J.A. Fang, H. Li, Finite-time synchronization of memristive neural networks with discontinuous activation functions and mixed time–varying delays, Neurocomputing 340 (2019) 99–109.
[38] S. Vong, C. Shi, Z. Yao, Exponential synchronization of coupled inertial neural networks with mixed delays via weighted integral inequalities, Int. J. Robust Nonlinear Control 30 (17) (2020) 7341–7354.
[39] H. Li, C. Li, T. Huang, D. Ouyang, Fixed-time stability and stabilization of impulsive dynamical systems, J. Frankl. Inst 354 (18) (2017) 8626–8644.
[40] J. Lu, B. Jiang, W.X. Zheng, Potential impacts of delay on stability of impulsive control systems, IEEE Trans. Automat. Contr. (2021), doi:10.1109/TAC.2021.3120672.
[41] B. Jiang, J. Lu, Y. Liu, Exponential stability of delayed systems with average-delay impulses, SIAM J. Control Optim. 58 (6) (2020) 3763–3784.
[42] S. Ding, Z. Wang, H. Zhang, Event-triggered stabilization of neural networks with time-varying switching gains and input saturation, IEEE Trans. Neural Netw. Learn. Syst. 29 (10) (2018) 5045–5056.
[43] S. Wu, X. Li, Y. Ding, Saturated impulsive control for synchronization of coupled delayed neural networks, Neural Netw. 141 (2021) 261–269.
[44] T. Yu, H. Wang, J. Cao, Y. Yang, On impulsive synchronization control for coupled inertial neural networks with pinning control, Neural Process. Lett. 51 (3) (2020) 1–6.
[45] Y.Y. Cao, Z. Lin, D.G. Ward, Anti-windup design of output tracking systems subject to actuator saturation and constant disturbances, Automatica 40 (7) (2004) 1221–1228.
[46] D. Ouyang, J. Shao, H. Jiang, S.K. Nguang, H.T. Shen, Impulsive synchronization of coupled delayed neural networks with actuator saturation and its application to image encryption, Neural Netw. 128 (2020) 158–171.
[47] J. Ma, S.S. Ge, Z. Zheng, D. Hu, Adaptive NN control of a class of nonlinear systems with asymmetric saturation actuators, IEEE Trans. Neural Netw. Learn. Syst. 26 (7) (2014) 1532–1538.
[48] Z. Yu, S. Li, Z. Yu, Adaptive neural control for a class of pure-feedback nonlinear time-delay systems with asymmetric saturation actuators, Neurocomputing, 173 (2016) 1461–1470.
[49] W. Si, X. Dong, F. Yang, Decentralized adaptive neural control for interconnected stochastic nonlinear delay-time systems with asymmetric saturation actuators and output constraints, J. Frankl. Inst 355 (1) (2018) 54–80.
[50] H. Wu, C. Li, Z. He, Y. Wang, Y. He, Lag synchronization of nonlinear dynamical systems via asymmetric saturated impulsive control, Chaos Solit. Fractals 152 (2021) 111290.
[51] R. Rakkiyappan, V.P. Latha, Q. Zhu, Z. Yao, Exponential synchronization of markovian jumping chaotic neural networks with sampled-data and saturating actuators, Nonlinear Anal.: Hybrid Syst 24 (2017) 28–44.
[52] Y. Chen, Z. Wang, B. Shen, H. Dong, Exponential synchronization for delayed dynamical networks via intermittent control: dealing with actuator saturations, IEEE Trans. Neural Netw. Learn. Syst. 30 (4) (2018) 1000–1012.
[53] J. Qi, C. Li, T. Huang, Stability of inertial BAM neural network with time-varying delay via impulsive control, Neurocomputing 161 (2015) 162–167.